A Thesis

On

Vibration Analysis of Carbon Nanotube Through Finite Element Method

Submitted in partial fulfillment of the requirement for the award of Degree of

Master of Engineering

IN

CAD/CAM & Robotics

Submitted By

DAVINDER SAINI

Roll No. 801081007

Under the Guidance of

Mr. DEVENDER KUMAR

Assistant Professor

Department of Mechanical Engineering

Thapar University, Patiala

DEPARTMENT OF MECHANICAL ENGINEERING

THAPAR UNIVERSITY

PATIALA-147004, INDIA

June-2012

DECLARATION

I hereby declare that the thesis entitled "**Vibration Analysis Of Carbon Nanotube Through Finite Element Method**" is an authentic record of my study carried out as requirement for the award of the degree of Master of Engineering (CAD/CAM & Robotics) at Thapar University, Patiala under the guidance of DEVENDER KUMAR, Assistant Professor, Department of Mechanical Engineering, Thapar University, Patiala during July 2011 to June 2012. The matter embodied in this report has not been submitted in part or full to any other university or institute for the award of any other degree.

(Davinder Saini)

Reg. No. 801081007

This is to certify that above declaration made by the student concerned is correct to the best of my knowledge & belief.

(Mr. DEVENDER KUMAR)
Assistant professor,
Department of Mechanical Engineering,
Thapar University, Patiala

Countersigned by:

(Dr. AJAY BATISH)
Professor and Head,
Department of Mechanical Engineering,
Thapar University,
Patiala-147004

(Prof. S.K.MOHAPATRA)
Dean, Academic Affairs,
Thapar University,
Patiala-147004

ACKNOWLEDGEMENT

I would like to express a deep sense of gratitude and thank profusely to my guide **Mr. DEVENDER KUMAR** for his sincere & invaluable guidance, suggestions and attitude, which inspired me to submit thesis in the present form. His dynamism and diligent enthusiasm have been highly instrumental in keeping my spirits high. His flawless and forthright suggestions blended with an innate intelligent application have crowned my task with success.

I am also thankful to **Dr. AJAY BATISH,** Professor and Head, Department of Mechanical Engineering for his encouragement and inspiration for execution of the thesis work.

I am also thankful to all my dear friends of Thapar University for the help regarding the finite element simulation used for the present study.

Dated: **DAVINDER SAINI**

Registration No.: 801081007

ABSTRACT

The primary motivation of the current research focuses on the ability to create simplified models that can accurately predict the structural and vibrational response of carbon nanotube structures undergoing different types of loading conditions. We have created a general process to make the carbon nanotube structures in different simulation software to do the finite element modeling and analysis. In this way, the mechanical characteristics regarding single-walled carbon nanotubes (SWCNTs) through Finite element modeling are computed.

A simplified finite element model is created for different types of SWCNTs & MWCNTs with varying input parameters like Charity, tube-length, tube-diameter and the geometries of the nanotubes are also altered through various beam cross-section employed for the construction of the C-C bonds. The current work contributes to the generation of different model responses to monitor the vibration signatures employing a wide range of parameter values and comparison of the results with the existing research. The ability to introduce variability in the parameters and boundary conditions without altering the capabilities and computational time in the model represents the main contribution of the thesis from the mechanical component.

ANSYS Software is used to do the finite element analysis of carbon nanotubes and PAYTHON language is used to generate the coordinates and the bonds for the ANSYS MECHANICAL APDL solver.

Findings explaining the output from the mechanical simulations are summarized. Furthermore, conceptual contributions for future work are listed to develop models capable of physically interpreting the characteristics of SWCNTs & MWCNTs.

LIST OF FIGURES

LIST OF TABLES

ABBREVIATIONS

C_h	Chiral Vector
T	Translational Vector
R	Symmetry Vector
a	Lattice constant of graphite
D	Diameter of carbon nanotube
SWCNT	Single wall carbon nanotube
MWCNT	Multi wall carbon nanotube
Θ	Chiral angle
0D	Zero Dimensional
1D	One Dimensional
2D	Two Dimensional
3D	Three Dimensional
d_R	Greatest common divisor
CNT	Carbon nanotubes
Pa	Pascal
GPa	Giga Pascal
TPa	Tara Pascal
U_i	Displacement component
N_{iK}	Shape Function at i^{th} element
D_K	Nodal displacement
ϵ	Strain
τ	Stress
$\mathcal{P}$	Potential energy
b_i	Body forces
T_i^o	Stress Tensor
vdW	Van der Waals

E	Young modulus
I	Second moment of inertia
f_i	Natural Frequency
D_o	Outer diameter
D_i	Inner Diameter
SEM	Scanning Electron Microscope
AFM	Atomic Force Microscope
TEM	Transmission Electron Microscope
a_{C-C}	Carbon-Carbon bond length
FE	Finite Element
IGES	Initial Graphics Exchange Specification
nm	Nanometer
pdb	Protein data bank
C-C	Carbon carbon atom
I_{xx}	Moment of inertia about x axis
I_{yy}	Moment of inertia about y axis
I_{zz}	Moment of inertia about z axis
T_{Ky}	Element Thickness in y direction
T_{Kz}	Element Thickness in y direction
Å	Armstrong
EX	Young Modulus
PRXY	Poisson Ratio
DENS	Density

INDEX

CHAPTER 1

INTRODUCTION TO NANOTECNOLOGY

1.1 Introduction To Nanotechnology

"A very succinct definition of nanotechnology is simply "engineering with atomic precision". Nanotechnology is the study and creation process of functional and useful materials, devices, and systems through control of matter at the nanometer scale, generally between 1 to 100 nanometers in at least one dimension. The study of physical properties of Nano scale materials have led to numerous new applications. The aim of nanotechnology is to make use of these properties and efficiently manufacture and generate larger structures with fundamentally new molecular organization.

Utilizing their properties at the nanoscale and bringing these properties to the macroscale are difficult tasks. For this reason, a new conceptual framework for nanotechnology development which takes into consideration the present scientific potential has been envisioned. It proposes an interdisciplinary approach spanning across applied physics, materials science, engineering, mechanics, electronics, and biology. The framework describes four generations of nanotechnology development. The first generation of nanotechnology products incorporates passive nanostructures and designed materials to perform one task. The second phase introduces active nanostructures for multitasking such as actuators, drug delivery devices, and sensors. The third generation features Nano systems with thousands of interacting components built from the bottom-up, rather than manufactured using top-down fabrication methods. Such achievements would lead to the fourth generation which is expected to combine heterogeneous molecular systems. From this point of view, the contemporary research performed in this area is not nanotechnology in the original meaning of the word. Realistically, the nanotechnology development could be considered at the end of the first generation. From this perspective, the synthesis of nanomaterial with controlled structure plays a crucial role in nanotechnology research towards the second generation of nanotechnology development.[1]

1.2 History

Carbon nanotubes had been discovered 30 years earlier, but had not been fully appreciated at that time. In the late 1950s, Roger Bacon at Union Carbide, found a strange new carbon fibre while studying carbon under conditions near its triple point. He observed straight, hollow tubes of carbon that appeared to consist in graphitic layers of carbon separated by the same spacing as the planar layers of graphite. In the 1970s, Morinobu Endo observed these tubes again, produced by a gas-phase process. Indeed, he even observed some tubes consisting in only a single layer of rolled-up graphite.

In 1991, after the discovery and verification of the fullerenes, Sumio Iijima[1] of NEC observed multiwall nanotubes formed in a carbon arc discharge, and two years later, he and Donald Bethune at IBM independently observed single-wall nanotubes – buckytubes. These pure carbon polymers could now be understood in the context of fullerenes, changing the perception of them to molecules, with all that special designation implies. Nanotubes had been fullerenized.[1].

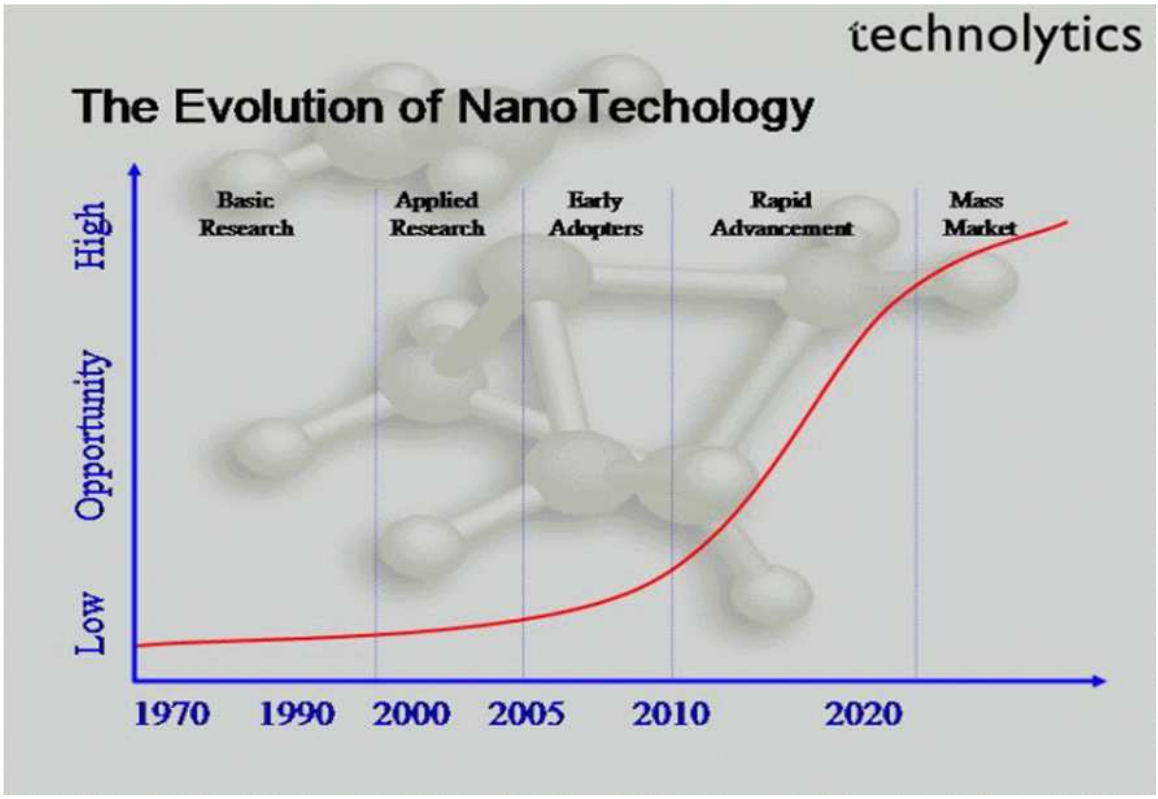

Figure 1.1: The Evolution of Nanotechnology [2]

A quite different approach to the nano scale starts from the microscopic world of precision engineering, progressively scaling down to ultra-precision engineering. The word "nanotechnology" was coined by Norio Taniguchi in 1983 to describe the lower limit of this process. Current ultrahigh-precision engineering is able to achieve surface finishes with a roughness of a few nanometers. This trend is mirrored by relentless miniaturization in the semiconductor processing industry. Ten years ago the focus was in the micrometer domain. Smaller features were described as decimal fractions of a micrometer. Now the description, and the realization, is in terms of tens of nanometers.

A third approach to nanotechnology is based on self-assembly. Interest in this arose because, on the one hand, of the many difficulties in making Drexler Ian assemblers, which would appear to preclude their realization in the near future, and on the other hand, of the great expense of the ultrahigh precision approach. The inspiration for self-assembly seems to have come from the work of virologists who noticed that pre-assembled components (head, neck, legs) of bacteriophage viruses would further assemble spontaneously into a functional virus merely upon mixing and shaking in a test-tube.

1.3 Carbon Nanomaterial

Nanomaterial cover various types of nanostructured materials which possess at least one dimension in the nanometer range. While most microstructure materials have similar properties to their bulk counterparts, the properties of materials with nanometer dimensions are significantly different from those of atoms and bulk materials. Carbon is a unique element due to its ability to form a variety of nanomaterial ranging from zero-dimensional (0D) fullerenes to one-dimensional (1D) conducting and semiconducting carbon nanotubes, and to two-dimensional (2D) semi metallic graphemes. These carbon based nanomaterial have remarkable physical properties and have received specific attention for a variety of applications. It clearly appears that carbon-based materials constitute a topic of huge scientific interest and great strategic importance, in which an interdisciplinary approach is necessary. Although the study of nanostructured carbon materials has recently undergone a steadily rapid development and keeps a fast moving research field, the investigation still

lacks in terms of fundamental understandings of the growth mechanisms and key factors responsible for the synthesis of carbon nanomaterial.

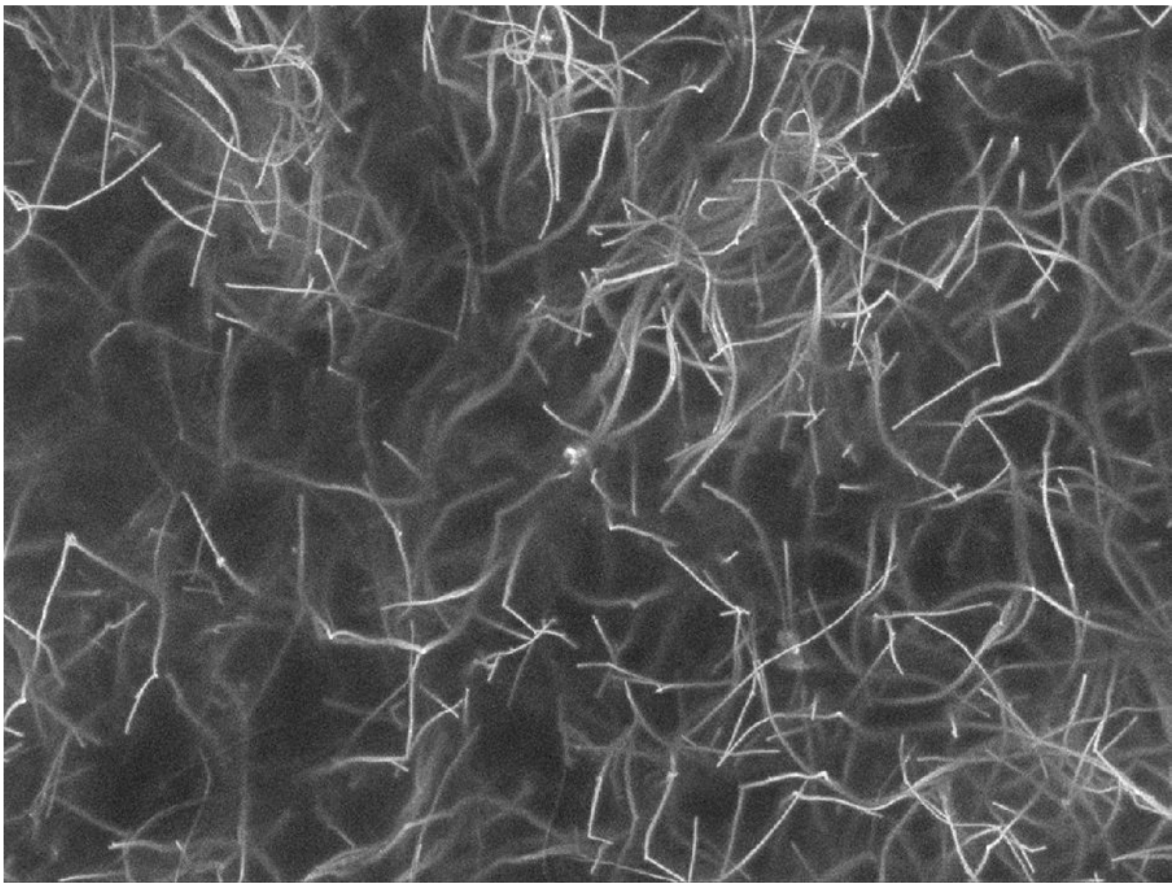

Fig1.2(Decorated Carbon Nanotubes)[3]

Moreover, because the carbon phase diagram is far from in-depth exploration, new forms of carbon are expected to be discovered. Carbon-based nanomaterials are currently considered a milestone in nanotechnology because they provide an accelerated scientific progress with many industrial applications. Achieving an enhanced degree of controllability and tuning capacity of material properties, would lead to the accomplishment of the ultimate Nano technological goal: the capability to design and manufacture various complex three-dimensional hierarchical assembly nanostructures and fabrication of self-assembly Nano engineered systems.

1.4 Carbon Nanotubes

A Carbon Nanotube is a tube-shaped material, made of carbon, having a diameter measuring on the nanometer scale. The graphite layer appears somewhat like a rolled-up chicken wire with a continuous unbroken hexagonal mesh and carbon molecules at the apexes of the hexagons.

Carbon Nanotubes have many structures, differing in length, thickness, and in the type of helicity and number of layers. Although they are formed from essentially the same graphite sheet, their electrical characteristics differ depending on these variations, acting either as metals or as semiconductors. [5]

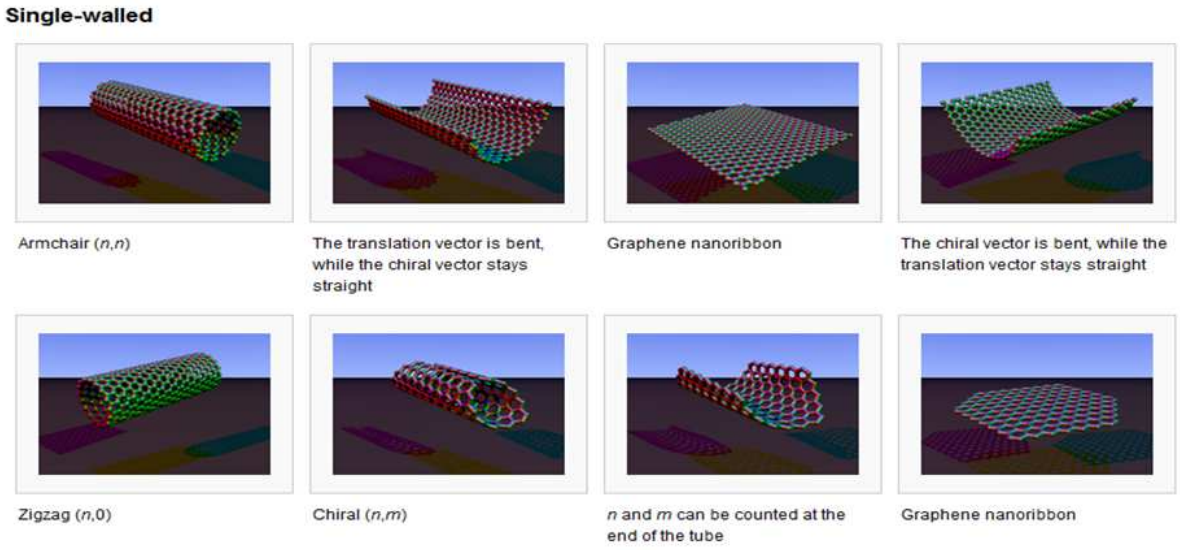

Figure 1.3: Different types of carbon Nanotubes [4]

As a group, Carbon Nanotubes typically have diameters ranging from 1 nm up to 50 nm. Their lengths are typically several microns, but recent advancements have made the nanotubes much longer, and measured in centimeters.

1.4.1 Structures of Carbon Nano Tubes

There are two types of CNTs: Single walled carbon nanotube (SWCNT) and multiwall carbon nanotube(MWCNT). MWCNTs are composed of co-axially situated SWCNTs of different radii. There are several ways to view a SWCNT. The most widely used is by rolling up grapheme sheet to form a hollow cylinder with or without end caps. [6, 7]

1.4.1.1 Structure of Single Wall Carbon Nanotube

Carbon nanotubes are viewed as hollow cylinders consisting of sp^2 bonds. The curvature presented in these structures causes σ-π rehybridization where the three σ bonds are considerably out of plane causing the π orbital to be more delocalized outside the tube. As a result, carbon nanotubes are mechanically stronger, electrically and thermally more conductive, and chemically and biologically more active than graphite.

SWCNTs can be viewed as hollow cylinders composed of a carbon hexagon pattern replicated throughout the entire structure. They are characterized by the chiral vector C_h defined by two integers (n, m) that are related to graphite vectors a1 and a2 as described by Eqn. 2.1: The atomic structure of carbon nanotubes depends on tube chirality[8]. The chiral vector C_h is defined as

$$C_h = na_1 + ma_2 \equiv (n, m). \qquad (1.1)$$

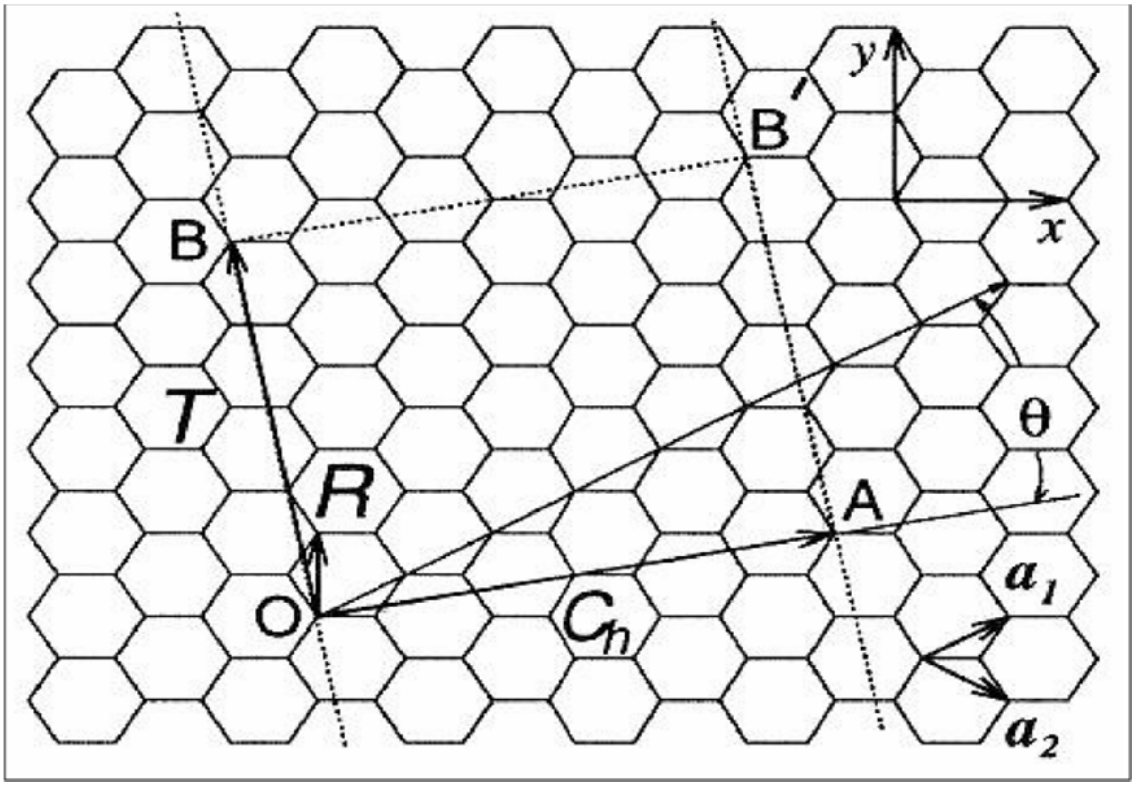

Figure 1.4: Unrolled lattice of a nanotube displaying the vectors OA and OB, which define the chiral vector C_h and translational vector T. R denotes the symmetry vector and rectangle OAB`B represents the unit cell of the nanotube.[6]

The structure of the carbon nanotube, as displayed in Fig. 1.1, is determined by the equator of the nanotube, that is, vector OA; which lies perpendicular to the tube axis. Conversely, the vector OB lies in the direction of the nanotube axis. By rolling the equivalent sites O, A, B, B` so that the points O and A as well as B and B` coincide allows the carbon nanotube structure to be created.[6]

The carbon nanotube has a diameter specified by:

$$D = |C_h|/\pi = \frac{a(n^2+nm+m^2)^{1/2}}{\pi} \qquad (1.2)$$

where a = $|a_1| = |a_2|$ and refers to the lattice constant of graphite. SWCNTs are classified in three different types: (1) armchair (n, n), (2) zigzag (n, 0), and (3) chiral (n, m). Examples of SWCNTs types are presented in Fig. 2.2, which are defined distinctively by the chiral angles. For the armchair and zigzag carbon nanotubes, the chiral angle Θ equals 30^O and 0^O, respectively, where n ≥ m. For the chiral SWCNT, Θ is defined by[8]

$$\theta = tan^{-1}[(\sqrt[2]{3}\ m/(m+2n)] \qquad (1.3)$$

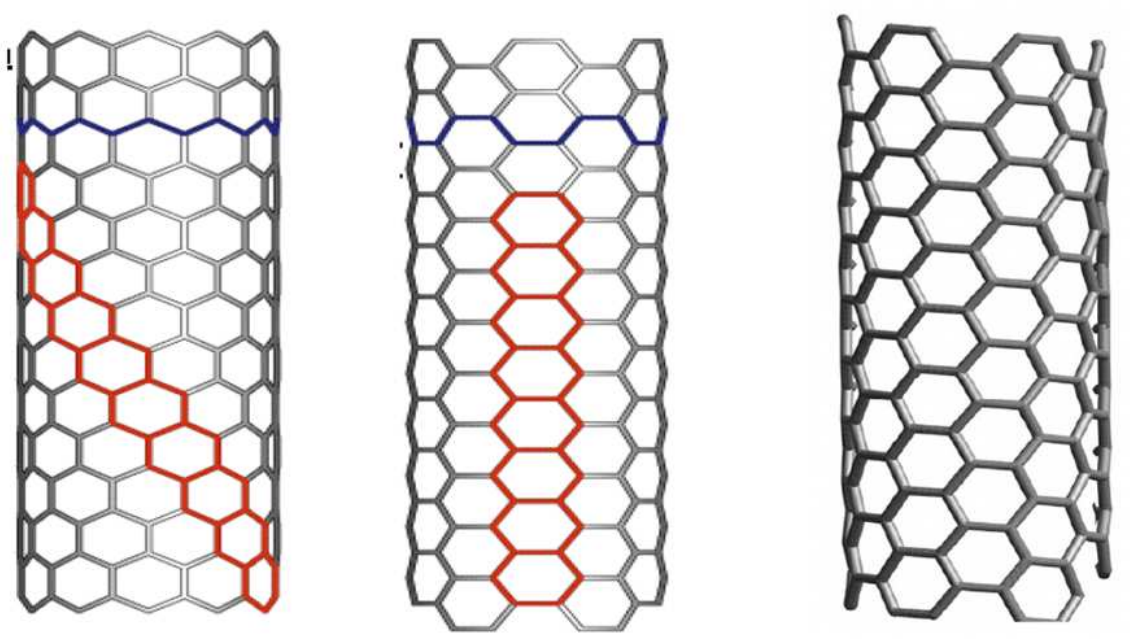

(a) (b) (c)

Figure 1.5: Classification of carbon nanotubes represent zigzag, armchair and chiral SWCNTs.

The translation vector T is defined as the unit vector of a 1D carbon nanotube. T is Parallel to the nanotube axis and perpendicular to the chiral vector C_h, as specified in Fig. 1.3. T can be expressed in terms of basis vectors a_1 and a_2 as

$$T = t_1 a_1 + t_2 a_2 \equiv (t_1, t_2) \quad (1.4)$$

Where t_1 and t_2 are integers determined by complying to orthogonally rules between T and C_h, that is from $C_h \cdot T = 0$. These integers are defined as

$$t_1 = \frac{2m+n}{d_R} \quad , \quad t_2 = -\frac{2n+m}{d_R} \quad (1.5)$$

where d_R represents the greatest common divisor of (2m + n) and (2n + m). Additionally, the length of the translational vector T is given by

$$T_1 = |T| = \frac{\sqrt{3}L}{d_R} \quad (1.6)$$

When the area of the nanotube unit cell $|C_h \times T|$ is divided by the area of the hexagon $|a_1 \times a_2|$, the number of hexagons per unit cell N is given as a function of n and m by

$$N = \frac{|C_h \times T|}{|a_1 \times a_2|} = \frac{2(m^2+n^2+nm)}{d_R} = \frac{2L^2}{a^2 d_R} = \frac{2LT}{\sqrt{3}a^2} \quad (1.7)$$

where L is the circumferential length of the carbon nanotube. The parameters L and d_R are governed by solution[6]:

$$L = 2\pi d_t, \quad (1.8)$$

$$d_R = \begin{cases} d \text{ if } n - m \text{ is not a multiple of } 3d \\ 3d \text{ if } n - m \text{ is a multiple of } 3d \end{cases} \quad (1.9)$$

Where d_t is the nanotube diameter and d is the greatest common divisor. The symmetry vector R (see Fig. 1.4) is another relevant component for the coordinate generation of carbon nanotube structures. Vector R is expressed in terms of its projections on the orthogonal vectors C_h and T of the nanotube unit cell. It can also be defined in terms of basis vectors a_1 and a_2 by

$$R = pa_1 + qa_2 \equiv (p, q) \quad (1.10)$$

Where p and q are the selected coefficient of the symmetry vector such that ($t_1 q - t_2 p = 1$). Other important parameters for the generation of carbon nanotubes are the lattice constant and intertube spacing, which depend on the tube diameter or radial direction. Experimental

and theoretical measurements agree that for a C−C bond length, C−C = 0.142nm or a = $|a_1|=|a_2|$ =0.246nm[8].

1.4.1.2 Structure of Multi Wall Carbon Nanotube

Multi-walled nanotubes (MWNT) consist of multiple rolled layers (concentric tubes) of graphite. There are two models that can be used to describe the structures of multi-walled nanotubes. In the Russian Doll model, sheets of graphite are arranged in concentric cylinders, e.g., a (0,8) single-walled nanotube (SWNT) within a larger (0,17) single-walled nanotube. In the Parchment model, a single sheet of graphite is rolled in around itself, resembling a scroll of parchment or a rolled newspaper. The interlayer distance in multi-walled nanotubes is close to the distance between graphene layers in graphite, approximately 3.4 Å. The Russian Doll structure is observed more commonly. Its individual shells can be described as SWNTs, which can be metallic or semiconducting. Because of statistical probability and restrictions on the relative diameters of the individual tubes, one of the shells, and thus the whole MWNT, is usually a zero-gap metal [4].

Double-walled carbon nanotubes (DWNT) form a special class of nanotubes because their morphology and properties are similar to those of SWNT but their resistance to chemicals is significantly improved. This is especially important when functionalization is required (this means grafting of chemical functions at the surface of the nanotubes) to add new properties to the CNT. In the case of SWNT, covalent functionalization will break some C−C double bonds, leaving "holes" in the structure on the nanotube and, thus, modifying both its mechanical and electrical properties. In the case of DWNT, only the outer wall is modified. DWNT synthesis on the gram-scale was first proposed in 2003 by the CCVD technique, from the selective reduction of oxide solutions in methane and hydrogen [4].

The telescopic motion ability of inner shells and their unique mechanical properties permit to use multi-walled nanotubes as main movable arms in coming Nano mechanical devices. Retraction force that occurs to telescopic motion caused by the Lennard-Johnes interaction between shells and its value is about 1.5 nN.

1.4.2 Growth and Synthesis of SWCNTs

SWCNTs are characterized by being sensitive to variations in the process parameters, including light intensity, process temperature, geometry, carrier gas type, pressure and flow conditions. Growth time for SWCNTs produced in laser and arc processes is about 10 ms under optimal conditions. Both arc ablation and laser processes produce carbon in the form of spallated graphitic particles and single-walled nanohorn aggregates. These factors directly affect the yield and properties of SWCNTs. The growth of carbon nanotubes can be accomplished through three methods: carbon vapor generated by arc discharge of graphite, carbon vapor generated by laser ablation of graphite, and the vapor growth method. The arc discharge method remains the easiest and most inexpensive method to obtain significant quantities of SWCNTs; however, the nanotubes are less pure than those produced by the laser ablation method.[9]

1.4.2.1 Arc Discharge Method for Producing SWCNTs

SWCNTs are produced via the arc process using covaporization of graphite and metal in a composite anode, commonly made by drilling an axial hole in the graphite rod and densely packing it with a mixture of metal and graphite powders. Ni/Y and Co/Ni are the most common catalysts utilized in SWCNT production. Thermogravimetric analysis (TGA) and near-infrared (NIR) spectroscopy are utilized to accurately determine the metal and SWCNT content in the arc material. These methods appear to be the most useful for analyzing arc-product composition and structure.

SWCNTs are generally organized in bundles consisting of a few dozen tubes, tightly compounded in a honeycomb lattice with an average separation between tube axes of approximately 1.7nm. Bundles are covered with an amorphous carbon layer of approximately 2-5 nm thick, which contains embedded fullerenes. The majority of tubes have diameters in the range of 1.2-1.5 nm and lengths reaching up to 5 μm in the Ni/Y system and 20 μm in the Co/Ni system. SWCNT diameters depend on the temperature of the catalytic site at which growth occurs. This temperature is regulated by many factors, including heating of the reaction zone with an externally controlled heat source. The mean diameter of the SWCNTs increases with the environment temperature [9].

1.4.2.2 Laser Ablation Method of Carbon-Metal Target for Producing SWCNTs

Implementing laser techniques for the production of SWCNTs can yield up to 70-90% by conversion of graphite [6]. There are two methods to scale up the SWCNT production using laser ablation: (1) the continuous wave laser-powder method of SWCNT synthesis, and (2) the ultrafast pulses from a free electron laser (FEL) method. The SWCNT abundance in a soot product is 20-40% while the tube diameter ranges from 1.2-1.3nm.

For the second method, light pulses at a repetition rate of 75 MHz are generated to vaporize the graphite-metal target. The SWCNT soot is collected on a cold surface at a rate of 1500 mg/ h. As a result, SWCNT bundles are produced from 8-200 nm thick with diameter and length ranging from 0.4-1 nm and 5-20 μm, respectively. Transmission electron microscope (TEM) is employed to verify the presence of ropes of SWCNTs consisting of bundles aligned along an axis. The SWCNTs are held in bundles by the van der Waals forces forming a 2D triangular lattice with a lattice constant of 1.7 nm; and an inter-tube separation of 0.315 nm [6].

1.4.2.3 Vapor Growth Method

The vapor growth method is beneficial since it is a continuous production of carbon nanotubes, which at optimal conditions can produce large quantities of these structures under relatively controlled conditions. The equipment necessary for the synthesis of carbon nanotubes is analogous to that used for vapor-grown carbon fibers. Carbon nanotubes generated by the vapor-growth method show poor crystallinity, which is improved after a heat treatment at 2500-3000^{o}C in argon gas.

Other methods have been developed for the synthesis of carbon nanotubes, including the use of carbon ion bombardment to create carbon whiskers, and the use of solar energy to achieve temperatures of 3000 K. Nevertheless, development of optimal and control synthesis process is required for the higher production of purified SWCNTs.

1.4.3 Purification of SWCNTs

Carbon nanotubes, produced by any method, contain impurities. These impurities are mostly catalyst metal particles and different forms of amorphous carbon. There have been developed

several post processing purification methods with the goal of removing the metal catalysts and other impurities.

The major impurity in carbon nanotubes are iron particles, which can be up to 30% by weight. The most effective procedure has been reported by Cinke et al. [10] by applying the high pressure CO disproportionation (HiPco) process [6]. The (HiPco) process is based on the decomposition of $Fe(CO)_5$ to form iron clusters for the catalytic production of SWCNTs from CO at about 1000^oC. The procedure consists of an acid treatment by removing the metal Filtration, washing with water, and drying in vacuum. It has been found that high vacuum heat treatment of HiPco tubes reduces Fe content to 2% while the diameter of SWCNTs increases substantially. Cinke et al. [10] utilize a two-step purification process for the HiPco SWCNTs, which reduces the iron content to less than 1%. Through this approach, a high resolution transmission electron microscopy (HRTEM) is implemented in the purification process to monitor the quality of SWCNTs.

Another technique to enhance the purification process in SWCNTs has been performed by Laborde-Lahoz et al [11]. The authors execute a two-step reflux process, which eliminates the catalytic particles in the SWCNTs, optimally disperse the carbon nanotubes, and oxide them through the addition of carboxylic functional groups, which help the SWCNTs adhere to the polymer matrix using covalent bonding.

Providing an overall explanation about the structure and formation of carbon nanotubes enable the study of simulation methods that are able to resemble and quantify the properties by these structures. As a result, the two following sections provide a detailed overview of the different atomistic simulations and Finite element methods employed for the study of the SWCNT properties.

1.4.5 Properties of Carbon Nanotubes

1.4.5.1 Strength

Carbon nanotubes are the strongest and stiffest materials yet discovered in terms of tensile strength and elastic modulus respectively. This strength results from the covalent sp2 bonds formed between the individual carbon atoms. In 2000, a multi-walled carbon nanotube was tested to have a tensile strength of 63 gigapascals (GPa). (For illustration, this translates into the ability to endure tension of a weight equivalent to 6422 kg on a cable with cross-section

of 1 mm2.) Further studies, conducted in 2008, revealed that individual CNT shells have strengths of up to 100 GPa, which is in good agreement with quantum/atomistic models. Since carbon nanotubes have a low density for a solid of 1.3 to 1.4 g/cm3, its specific strength of up to 48,000 kN·m·kg−1 is the best of known materials, compared to high-carbon steel's 154 kN·m·kg−1.

Under excessive tensile strain, the tubes will undergo plastic deformation, which means the deformation is permanent. This deformation begins at strains of approximately 5% and can increase the maximum strain the tubes undergo before fracture by releasing strain energy.

Although the strength of individual CNT shells is extremely high, weak shear interactions between adjacent shells and tubes leads to significant reductions in the effective strength of multi-walled carbon nanotubes and carbon nanotube bundles down to only a few GPa's. This limitation has been recently addressed by applying high-energy electron irradiation, which crosslinks inner shells and tubes, and effectively increases the strength of these materials to 60 GPa for multi-walled carbon nanotubes and 17 GPa for double-walled carbon nanotube bundles.

1.4.5.2 Electrical Properties

Because of the symmetry and unique electronic structure of graphene, the structure of a nanotube strongly affects its electrical properties. For a given (n,m) nanotube, if n = m, the nanotube is metallic; if n − m is a multiple of 3, then the nanotube is semiconducting with a very small band gap, otherwise the nanotube is a moderate semiconductor. Thus all armchair (n = m) nanotubes are metallic, and nanotubes (6,4), (9,1), etc. are semiconducting.

However, this rule has exceptions, because curvature effects in small diameter carbon nanotubes can strongly influence electrical properties. Thus, a (5,0) SWCNT that should be semiconducting in fact is metallic according to the calculations. Likewise, vice versa-- zigzag and chiral SWCNTs with small diameters that should be metallic have finite gap (armchair nanotubes remain metallic). In theory, metallic nanotubes can carry an electric current density of 4 × 109 A/cm2, which is more than 1,000 times greater than those of metals such as copper, where for copper interconnects current densities are limited by electromigration.

Multiwalled carbon nanotubes with interconnected inner shells show superconductivity with a relatively high transition temperature Tc = 12 K. In contrast, the Tc value is an order of

magnitude lower for ropes of single-walled carbon nanotubes or for MWNTs with usual, non-interconnected shells[12].

1.4.5.3 Hardness

Standard single-walled carbon nanotubes can withstand a pressure up to 24GPa without deformation. They then undergo a transformation to super hard phase nanotubes. Maximum pressures measured using current experimental techniques are around 55GPa. However, these new super hard phase nanotubes collapse at an even higher, albeit unknown, pressure. The bulk modulus of superhard phase nanotubes is 462 to 546 GPa, even higher than that of diamond (420 GPa for single diamond crystal)[4].

1.4.5.4 Toxicity

The toxicity of carbon nanotubes has been an important question in nanotechnology. Such research has just begun. The data are still fragmentary and subject to criticism. Preliminary results highlight the difficulties in evaluating the toxicity of this heterogeneous material. Parameters such as structure, size distribution, surface area, surface chemistry, surface charge, and agglomeration state as well as purity of the samples, have considerable impact on the reactivity of carbon nanotubes. However, available data clearly show that, under some conditions, nanotubes can cross membrane barriers, which suggests that, if raw materials reach the organs, they can induce harmful effects such as inflammatory and fibrotic reactions[4].

1.5 Finite Element Modeling of Carbon Nanotubes

The Finite element method provides an approximate solution to the equations of the theory of elasticity. The main concept of this method is to divide the body into small parts named elements. The displacement field is then approximated in each element through interpolation between the values of the displacement at specific points on the element called nodes. The displacement field, which is assumed to be continuous, is then substituted into the potential energy expression. This condition generates a set of linear algebraic equations for the nodal displacements through the condition of minimum potential energy. The elements are numbered e = 1,2,3, … M, and the unknown nodal displacements are n=1,2,3, … N,

Consider one element and one displacement component ui within an element. The component U_i is dependent on the nodal displacements D_K for that element. However, the dependency relies only on the displacements at nodes falling within the element or on its boundary. The displacement component is described through the linear relation

$$U_i(x) = \sum_{K \epsilon I_m} N_{iK}(x) D_K \qquad (1.11)$$

where I_m refers to the set of nodal displacements for the m^{th} element, i = 1,2,3 for 3D problems, and N_{iK} are the shape functions for the element.

The shape functions must provide continuity to the generated displacement field, and be approximated to the true solution so that the error tends to zero as the element size tends to zero. Therefore, these functions must comply with the following:

(1) element boundary continuity for arbitrary nodal displacements

(2) exact representation of constant strain in the element.

Through the shape functions, the strains are determined by

$$\epsilon_{ij} = \sum_{K \epsilon I_m} A_{ijK} D_K \qquad (1.12)$$

Where A_{ijK} refers to

$$A_{ijK} = \frac{1}{2}\left(\frac{\partial N_{ik}}{\partial x_j} + \frac{\partial N_{jk}}{\partial x_i}\right) \qquad (1.13)$$

The calculated stress is given by

$$\tau_{ij} = l_{ij} + \sum_{K \epsilon I_m} B_{ijK} D_K \qquad (1.14)$$

where the cofficient B_{ijK} is described as

$$B_{ijK} = c_{ijkm} A_{kmK} \qquad (1.15)$$

where C_{ijkm} and l_{ij} are characteristic of the structure.

For each element a function A(ε) is defined as

$$A(\varepsilon) = \frac{1}{2} c_{ijkm} + l_{ij\varepsilon ij} \qquad (1.16)$$

$$= \sum_{K \epsilon I_m} \quad \sum_{M \epsilon I_m} \frac{1}{2} A_{ijK} B_{ijM} D_k D_m + \sum_{K \epsilon I_m} l_{ij} A_{ijK} D_K \qquad (1.17)$$

in which indices K and M range over the index set for the particular element.

Considering the potential energy, the elements divide the region υ into sub-regions υm. Let Sm indicate the part of the boundary of the sub-region υm position on the loaded exterior surface. Then, the potential energy becomes

$$\mathcal{P} = \sum_{m=1}^{M} \mathcal{P}_m = \sum_{m=1}^{M} \left(\int_{\upsilon_m} [A(\epsilon) - b_i u_i] dV - \int_{S_m} T_i^o U_i dA \right) \quad (1.18)$$

where b_i represents the body forces per unit mass and T_i^o is the stress tensor.

Replacing Eqns. 1.11 and 1.17 in Eqn. 1.18, the potential energy for the element becomes

$$\mathcal{P} = \sum_{I,J \epsilon I_m} \frac{1}{2} k_{Ij}^m D_i D_j - \sum_{I \epsilon I_m} f_I^m D_I \quad (1.19)$$

Where k_{Ij}^m and f_I^m are defined as

$$k_{Ij}^m = \int_{\upsilon_m} B_{kiI} A_{kij} dV \quad (1.20)$$

$$f_I^m = -\int_{\upsilon_m} l_{ki} A_{ki} dV + \int_{\upsilon_m} b_k N_{kl} dV + \int_{S_m} T_{ik}^o N_{kI} dA \quad (1.21)$$

As a result, the potential energy of the body becomes a summation as shown in Eqn. 1.19 I and J depends on the element m. To perform the sum on m, Eqn. 1.19 can be extended to all displacement parameters by defining k_{ij}^m to be zero for all I and J not included in the set I_m, Combining Eqn. 1.18 and Eqn. 1.19, the total potential equation simplifies to

$$\mathcal{P} = \sum_{I=1}^{N} \sum_{J=1}^{N} \frac{1}{2} K_{IJ} D_I D_J - \sum_{J=1}^{N} F_J D_J \quad (1.22)$$

Where K_{IJ} and F_J represent the stiffness and force matrix for N degrees of freedom, respectively. These are defined as

$$K_{IJ} = \sum_{m=1}^{M} k_{IJ}^m \quad (1.23)$$

$$F_I = \sum_{m=1}^{M} F_I^m \quad (1.24)$$

The system equations are solved by minimizing the potential energy, that is, $\frac{\partial \mathcal{P}}{\partial D_I} = 0$, by applying this condition, a set of N equations is generated with N unknowns,

$$\sum_{J=1}^{N} K_{ij} D_j = F_I \quad (1.25)$$

Eqn. 1.25 is solved numerically for D_J . Therefore, displacement, strain, and stress fields for an element are calculated using Eqns. 1.11 and 1.14 [13].

Through the solution of this system of equations, carbon nanotube structures are modeled in a continuum environment, which focuses on developing a nanoscale continuum model to simulate the mechanical behavior of these structures.

CHAPTER 2

LITERATURE REVIEW

2.1 Introduction

The extraordinary characteristics of carbon nanotubes (CNTs) give them potential in numerous applications and open an incredible range of all kind of applications. The combination of exceptional mechanical and physical properties makes CNTs prospective candidates for reinforcement of polymer matrix composite systems. The fact that the inclusion of even small amounts of nanomaterial coupled with appropriate processing steps appears to significantly improve mechanical properties have catapulted carbon nanotube to being one of the first practical application areas of nanotechnology. The mechanical properties of CNT depend on many factors. Since it is difficult to control these factors experimentally, modeling and simulations could provide crucial insight and design guidance.

2.2 Literature Review

Since the discovery of carbon nanotube by **Iijima**[1] , researchers put their utmost efforts to find its property of the same. Carbon nanotubes show finds a wide range of applications in Physics and engineering. However, understanding the CNT is still a mystery because of its Nano size which prevents from physical experiments. Researchers tried to find the properties of single walled and multiwall carbon nanotube properties, this lead to many theories regarding Carbon nanotubes and followed by the many results regarding the same parameter.

R. Saito *et al.* [6] has published introductory textbook for researchers from various fields of science who wish to learn about carbon nanotubes. The field is still at an early stage, and progress continues at a rapid rate. This book focuses on the basic principles behind the physical properties and gives the background necessary to understand the recent developments. Some useful computational source codes which generate coordinates for carbon nanotubes are also included in the appendix.

K.I. Tserpes and P. Papanikos [7] has generated FE model for armchair, zigzag and chiral SWCNTs has been proposed. The model development is based on the assumption that CNTs, when subjected to loading, behave like space-frame structures. As the FE model comprises small number of elements, it performs under minimal computational time by requiring minimal computational power. This advantage, in combination with the modeling abilities of the FE method, extends the model applicability to SWCNTs with very large number of atoms as well as to MWCNTs, other carbon-related Nano-structures and moreover, to CNT-based Nano-composites. The model has been used to investigate the effect of wall thickness, diameter and chirality on the elastic moduli (Young's modulus and shear modulus) of SWCNTs. Armchair, zigzag and two series of chiral SWCNTs have been included in the investigation. For the values of wall thickness used in the literature, the obtained values of Young's modulus agree very well with the corresponding theoretical results and many experimental measurements. The FE model results suggest that Young's modulus is inversely proportional to the wall thickness. Dependence of elastic moduli to diameter and chirality of the nanotubes has been also found. With increasing tube diameter, the elastic moduli of all SWCNTs increase. The Young's modulus of chiral SWCNTs is found to be larger than that of armchair and zigzag SWCNTs. The presented results demonstrate that the proposed FE model may provide a valuable tool for studying the mechanical behavior of CNTs and Nano composites.

J. Han. [8] has taken a comprehensive look at this diverse and dynamic subject, Carbon Nanotubes: Science and Applications describes the field's various aspects, including properties, growth, and processing techniques, while focusing on individual major application areas. Well-known authors who practice the craft of carbon nanotubes on a daily basis present an overview on structures and properties, and discuss modeling and simulation efforts, growth by arc discharge, laser ablation, and chemical vapor deposition. Applications become the focal point in chapters on scanning probe microscopy, carbon nanotube-based diodes and transistors, field emission, and the development of chemical and physical sensors, biosensors, and composites.

A.P. Moravsky *et al.*[9] discuss that SWCNTs are generally organized in bundles consisting of a few dozen tubes, tightly compounded in a honeycomb lattice with an average separation between tube axes of approximately 1.7nm. Bundles are covered with an amorphous carbon layer of approximately 2-5 nm thick, which contains embedded fullerenes. The majority of tubes have diameters in the range of 1.2-1.5 nm and lengths reaching up to 5 μm in the Ni/Y system and 20 μm in the Co/Ni system. SWCNT diameters depend on the temperature of the catalytic site at which growth occurs. This temperature is regulated by many factors, including heating of the reaction zone with an externally controlled heat source. The mean diameter of the SWCNTs increases with the environment temperature

M. Cinke *et al.*[11] discuss that the (HiPco) process is based on the decomposition of $Fe(CO)^5$ to form iron clusters for the catalytic production of SWCNTs from CO at about 1000^oC. The procedure consists of an acid treatment by removing the metal Filtration, washing with water, and drying in vacuum.

P. Laborde-Lahoz *et al.*[11] execute a two-step reflux process, which eliminates the catalytic particles in the SWCNTs, optimally disperse the carbon nanotubes, and oxide them through the addition of carboxylic functional groups, which help the SWCNTs adhere to the polymer matrix using covalent bonding.

C. Kittel *et al.*[12] discuss that by exploring the electrical properties of carbon nanotubes, it is possible to explore the noticeable distinctions regarding conductivity between metals and semiconductors presented in carbon nanotube structures. It is possible to observe the band gap differences between metals and semiconductors. For instance, in metals, 10%-90% of bands are partially filled. On the other hand for semiconductors, one or two bands are slightly filled (or empty)

E.H. Dill [13] described the direct stiffness method of finite element analysis is by now well established and widely used for the solution of small displacement, elastic structural problems. Various types of element have been developed and general purpose computer programs now exist which can be used with any element for the solution of large-scale

problems. Such general purpose programs have great practical advantages because of the rapidity with which they can be applied to any particular problem. Since the establishment of the method, there has been much interest in extensions for nonlinear analysis. The nonlinearities arise from two distinct sources: constitutive nonlinearities and geometric nonlinearities, the latter being due to large displacements. The most commonly used nonlinear material is the elastic-plastic material, and for this material the linearity of the incremental stress-strain law forms the basis of the equations, its most direct application being in the incremental type solution, where the solution is built up as a series of linear increments.

R. Ansari *et al.*[14] compared the results of molecular dynamics (MD) and continuum shell model and deduced that the continuum model provides a remarkably accurate ‘‘roadmap’’ of nanotube behavior beyond Hooke’s law if model parameters are properly chosen. classical continuum shell model allowing for the van der Waals (vdW) interlayer interactions to study the buckling of single- and multi-walled carbon nanotubes under axial compression and external pressure. By studying the torsional and bending buckling of multi-walled carbon nanotubes using solid shell elements we can employ the molecular structural mechanics approach to model the elastic buckling of single- and multi-walled carbon nanotubes under axial compression and bending loading. Analytical solutions can be obtained for the critical buckling strain of single-walled carbon nanotubes based on a molecular mechanics model. They reported that zigzag tubes are more stable than armchair tubes of the same diameter. Deriving explicit formulas for the van der Waals (vdW) interaction between any two layers of a multi-walled carbon nanotube (CNT), which are modeled by elastic shells. Based on their results, vdW interaction will lead to a higher critical buckling load in multi-walled CNTs.

Anand Y.Joshi *et al.*[15] discuss principle of mass detection using resonators is based on the fact that the resonant frequency is sensitive to the resonator mass, which includes the self-mass of the resonator and the mass attached on the resonator. The change of the mass attached on the resonator can cause a shift of the resonant frequency. The key issue of mass detection is in quantifying the change in the resonant frequency due to the added mass.

Continuum mechanics method has been successfully applied to analyze the dynamic responses of individual CNTs.

Based on the Euler–Bernoulli beam model, the equation of motion of a free vibration of a rod in the limit of small amplitude is governed by the wave equation

$$EI\frac{\partial^4 w}{\partial x^4} + \rho A\frac{\partial^2 w}{\partial t^2} = 0$$

where E is the young's modulus, I the second moment of the cross– sectional area A and r the density of the beam material. The natural mechanical resonant frequency is induced in a bridged carbon nanotube when the applied frequency approaches the resonant frequency. Theoretically, the resonant frequency depends on the nanotube outer diameter, the inner diameter, the length, the density and the bending modulus of the nanotube, i.e.

$$f_i = \frac{\beta_i^2}{8\pi}\sqrt{\frac{(D_0^2 + D_i^2)E}{\rho L^4}}$$

where β1=4.730041, β2=7.853205, β3=10.995608 and β4=14.137165 for the 1st, 2nd, 3rd and 4th harmonics ,respectively. This study uses a continuum mechanics method with commercial FEM software to conduct the vibration analysis of a SWCNT approximated by a shell model with thickness. The resonant frequency and the mode shapes of the SWCNT are simulated using a bending model.

Mira Mitraa *et al*.[16] has studied the wave propagation in multi-walled carbon nanotubes using a continuum shell model based on Flugge theory. The modeling is done using the wavelet based spectral finite element which is ideal for wave propagation analysis in finite dimension waveguides of relatively high complexities. Here, MWNT is modeled as concentric cylinders coupled through interlayer vander walls interaction forces. The formulated wavelet based numerical scheme allows both frequency and time domain analysis unlike the existing Fourier transform based solution which are restricted to the study of dispersion relation and wave amplitudes. Here, WSFE is developed for a MWNT with arbitrary number of walls. First, the method is used to obtain the spectrum relation i.e. the wavenumber plots for a single, double and three walled carbon nanotubes. Several wave properties of MWNT can be extracted from this study, one being the cut-off frequency band

exhibited by the circumferential wave mode. This is an important observation as this property may be utilized to design a band gap filter. Apart from this, the wave speeds has also be studied for a single walled carbon nanotubes and the values have been validated with the experimental and atomistic simulation results available in literature. Finally, the model is used to simulate the axial, circumferential and radial wave responses in time domain which include the natural frequencies, snapshots of wave propagation in SWCNT and the time history of the wave transmission in three walled carbon nanotubes.

S.K. Georgantzinos *et al.*[17] developed numerical tool capable of predicting the mechanical behavior of SWCNT reinforced rubber has been developed. The formulation is based in a micromechanical, non-linear, multi-scale finite element approach and utilizes a Mooney–Rivlin material model for the rubber and takes into account the atomistic nanostructure of the nanotubes. The interfacial load transfer characteristics were parametrically approximated via the use of joint elements of variable stiffness. The case of rigid attachment between the two phases was also investigated. The computed composite stress–strain behaviors under pure tension show definite advantages that arise by the SWCNT reinforcement addition. The SWCNTs improve significantly the composite strength and toughness especially for higher volume fractions. Simultaneously, the absorption energy characteristics of the rubber material are maintained in the composite. Having as a basis the proposed method the mechanical response of rubber materials filled with SWCNTs with more complicated arrangement and nanostructure i.e. Nano textiles and Nano cords may be predicted in a future work.

S. Rajasekaran *et al.*[18] developed finite element model is developed for static and free vibration analysis of CNTs. The major advantages of the approach are the simplicity of the concept and the improved computational efficiency for analyzing the mechanical properties. The results obtained are compared with the existing methodologies and are found to be satisfactory. Also the Differential Quadrature method was found to be simpler for carrying out the analysis. The single beam model fails to represent the behavior of individual tubes and the relative deformation between adjacent tubes. In the multiple beam model, the deflections of the adjacent tubes are coupled due to the presence of Van der Waals forces.

Since the Nanotubes are treated individually in the multi-beam model, the end conditions can therefore be described individually. Here the concept of spring is introduced which actually represents the Van der Waal forces. The finite element analysis is performed using Matlab and the results are verified to have a check on the accuracy using the symbolic processing tool Mathematica. The deformations, buckling and vibrational analysis were carried out for single and Multi Walled Carbon Nanotubes.

Aleksander Muc [19] has interest in developing and modeling macroscale structures made CNTs has lead to the use of identification techniques to model their effective mechanical properties. For the identification purposes 3D space-frame finite element model is developed based on the consistent molecular mechanics formulations and employing Eigen frequency analysis for orthotropic thin shells. Two forms of the interatomic potentials are considered: the modified Morse potential and REBO potential. The proposed models are able to investigate the longitudinal and circumferential Young's moduli for various CNT configurations. Comparison of our results with those of available references shows that the present models are highly effective and capable of providing reasonable predictions for Young's modulus. The detailed investigations shows that the axial (longitudinal) Young's modulus is CNT dominated, while all properties associated with the transverse to CNT directions are less significant but cannot be neglected or eliminated.
Using the proposed model it is possible to explain the influence of the CNTs geometry and structure on Young's moduli. In this way it gives an opportunity for the optimal design of carbon nanostructures exploiting the knowledge of their transversely isotropic or orthotropic mechanical properties. It is worth to note again that the proposed description of carbon nanotubes as orthotropic bodies is completely consistent with micromechanical homogenization theory of composite materials or of skeletal or space-frame shell structures constituting (or being) in fact the structure of nanotubes. The identical identification method may be successfully used in the prediction of the effective mechanical properties for multiwall carbon nanotubes or for Nano composites reinforced with CNTs.

P. Zhang *et al*. [20] & [21] described that a nanotube can be modeled as a continuum solid beam tension, bending, or torsional forces, it is reasonable to model the nanotube as a frame

or shell-like structure, then the mechanical properties of such a structure can be obtained by classical continuum mechanics or finite element method. Thanks to the uncertainty of the CNT wall thickness Which again lead to many theories and in turn paved for many results, ranged from about 1.0 to 5.5 TPa a modulus value can be found from the researchers work. We have developed a finite element model of SWNTs and consequently estimated their mechanical property namely Young's modulus.

N. Khandoker *et al.***[22]** has discussed that individual multi walled Carbon Nanotubes (CNTs) exhibit exceptional strength and stiffness. However, large scale constructs of directly spinnable CNTs (such as yarns) has reached only a few percent of their potential. To improve their performances in such scale, it is important to understand the stress-strain characteristics and failure modes of individual CNTs. This paper reports the experimental tensile strength of spinnable multiwall carbon nanotubes (MWCNT). These experiments were conducted using a Nano tensile testing stage inside Scanning Electron Microscope (SEM) chamber. An Atomic Force Microscope (AFM) tip with known force constant was used as a Nano manipulator and as s force transducer to measure the desired mechanical properties. Transmission Electron Microscope (TEM) images were used to accurately measure the diameter of CNT samples. The fracture strength was calculated using the determined applied force and the diameter of the CNT. Fracture strength in relations to number of failed walls, pullout (sword/sheath) behavior and angle of stress are studied. It was found that the tensile strength of the tested spinnable CNTs were at least 20 to 90 Gpa with a mean value of 48 Gpa considering a solid cross sectional area.

R. Chowdhury *et al.*[23] discuss that the potential of SWCNT as a mass sensor is explored. CNTs are modeled by continuum based approach. Both cantilevered and bridged CNTs are investigated. The relationship between the resonant frequency and the attached mass is established using the Euler–Bernoulli beam theory. Using this relationship, a general closed-form nonlinear sensor-equation has been derived for the detection of the mass of biological objects attached to the CNT. The physical basis of the sensor is that the attached mass causes a frequency-shift. A simple linear approximation of the nonlinear sensor-equation has been

given. The accuracy of both the exact and the linear approximation has been verified using a detailed hi-fidelity finite-element simulation. It was observed that the proposed sensor-equations work reasonably well when the length of the bacteria is more than 1 nm for both cantilevered and bridged configurations.

B. Liu *et al*. [24] have developed an accurate atomic-scale finite element method AFEM that has exactly the same formal structure as continuum finite element methods, and therefore can seamlessly be combined with them in multiscale computations. The AFEM uses both first and second derivatives of system energy in the energy minimization computation. It is faster than the standard conjugate gradient method which uses only the first order derivative of system energy, and can thus significantly save computation time especially in studying large scale problems. Woven nanostructures of carbon nanotubes are proposed and studied via this new method, and strong defect insensitivity in such nanostructures is revealed. The AFEM is also readily applicable for solving many physics related optimization problems.

2.3 LITERATURE GAP

After doing detailed study of Literature on Vibrations of carbon nanotubes using Finite Element Method it is observed that:

- It's is very difficult to draw the exact shape of carbon nanotube in any simulation software.
- There is no single simulation software in which we can do straightway do analyses. Many authors have generated their own code for nanotube modeling which have been kept secret for reader. So we have created a generalized process to create any carbon nanotube structure and a vibration analysis of same has been done.
- It's has also been observed that lots of analyses has been done by taking tube diameter, tube length and chirality as parameter but not much work has been done by taking element type and element shape as varying parameter. Carbon-Carbon bond can be represented by rectangular, circular and irregular sections.

CHAPTER 3

METHODOLOGY

After doing detailed study of Literature on mechanical properties of carbon nanotubes, it is summarized that many experiments and analysis have been done to represent the vibration signature of carbon nanotubes, by varying tube structure, tube diameter, tube length, and loading conditions. Ansys Mechanical APDL 13.0 software will be used to simulate and analyze the vibrational behavior of carbon nanotubes by varying tube structure, tube diameter, tube length, and loading conditions. Nanotube Modeler 1.6.3 is used to draw the basic geometry of carbon nanotube and Wing IDE is used to execute the Python Script to convert .pdb file into ansys pre- processor script.

3.1 Finite Element Analysis

CNTs carbon atoms are bonded together with covalent bonds forming an hexagonal lattice. These bonds have a characteristic bond length a_{C-C} and bond angle in the 3D space. The displacement of individual atoms under an external force is constrained by the bonds. Therefore, the total deformation of the nanotube is the result of the interactions between the bonds. By considering the bonds as connecting load-carrying elements, and the atoms as joints of the connecting elements i.e.nodes, CNTs may be simulated as space-frame structures.

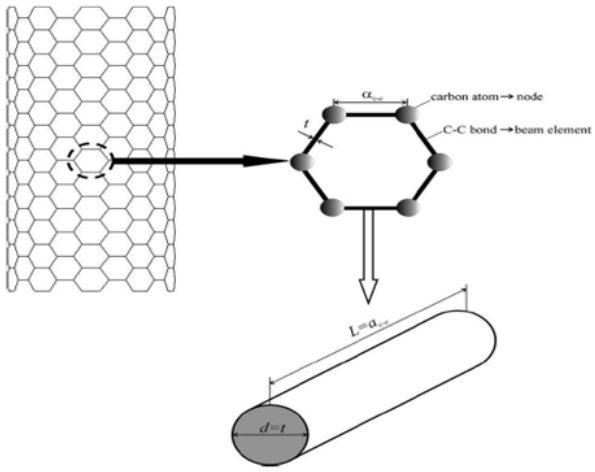

Figure 3.1 Representation of Carbon Nanotube in wireframe model with nodes and elements

By treating CNTs as space-frame structures, their mechanical behavior can be analyzed using classical structural mechanics methods. In this work, a 3D FE model able to assess the mechanical properties of SWCNTs is proposed.

3.1.1 Modeling of Carbon Nanotube

Our main aim is to create the wireframe structure of carbon nanotube in ansys software with accuracy. Ansys Mechanical APDL 13.0 can read only IGES format for external geometry importation and its very lengthy process to create a nanotube in any modeling software.

So we generalized the process of making structure of carbon nanotubes in ansys which contains following steps:

a) Creating desired model in Nanotube modeler.

b) Conversion of pdb file to Ansys pre-processor script.

c) Drawing model into Ansys .

3.1.1.1 Creating Model in Nanotube Modeler

Nanotube Modeler is a professional application designed to enable you to generate coordinates for nanotubes. Generated geometries may be viewed using the integrated viewer or by calling a viewer program of your choice.

Input Parameters requires to draw a nontube are:

Table 1: Input Parameters of Carbon Nanotube

Serial No.	Parameter	Symbol	Units
1	Chirality	(n,m)	No units
2	Tube Length	*l*	armstrrong
3	Tube Diameter	D	armstrrong
4	Tube Distortion	T_x, T_y, T_z, Θ	Armstrrong,radians

Nanotube Modeler can export the geometry in different type of geometries.

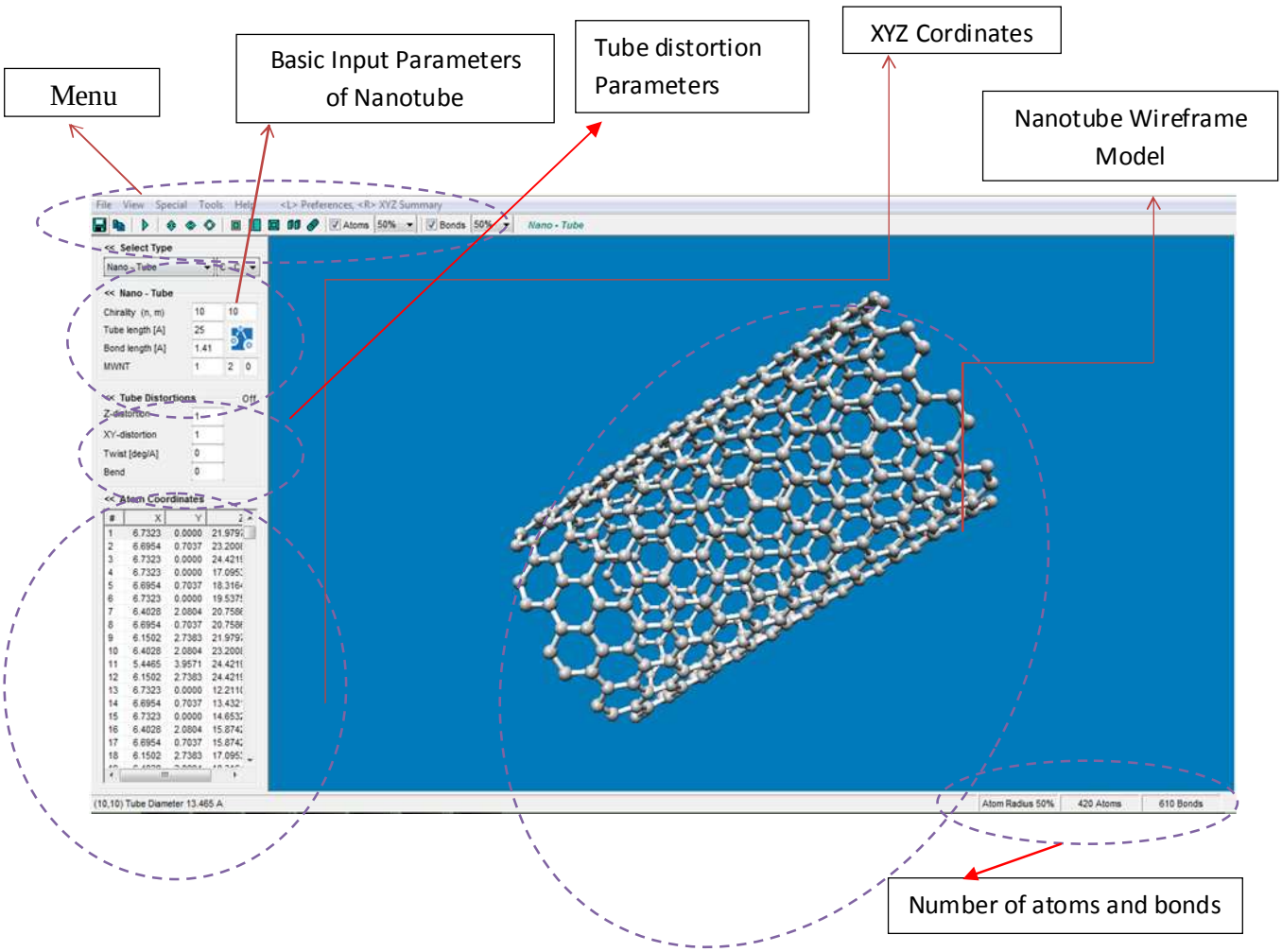

Figure 3.2: General Windows Layout for Nanotube Modeler

3.1.2 Generation of Compatible Model

The model which is generated by Nanotube Modeler cannot be imported to Ansys by any means so we have to generate the new model in Ansys using X-Y-Z coordinates and bond information. All the desired information about the carbon nanotube generated in Nanotube modeler can be saved as .pdb format.

3.1.2.1 PDB Format Description

The Protein Data Bank (pdb) file format is a textual file format describing the three dimensional structures of molecules held in the Protein Data Bank. The pdb format accordingly provides for description and annotation of protein and nucleic acid structures including atomic coordinates, observed side chain rotamers, secondary structure assignments, as well as atomic connectivity. Structures are often deposited with other molecules such as water, ions, nucleic acids, ligands and so on, which can be described in the pdb format as well.

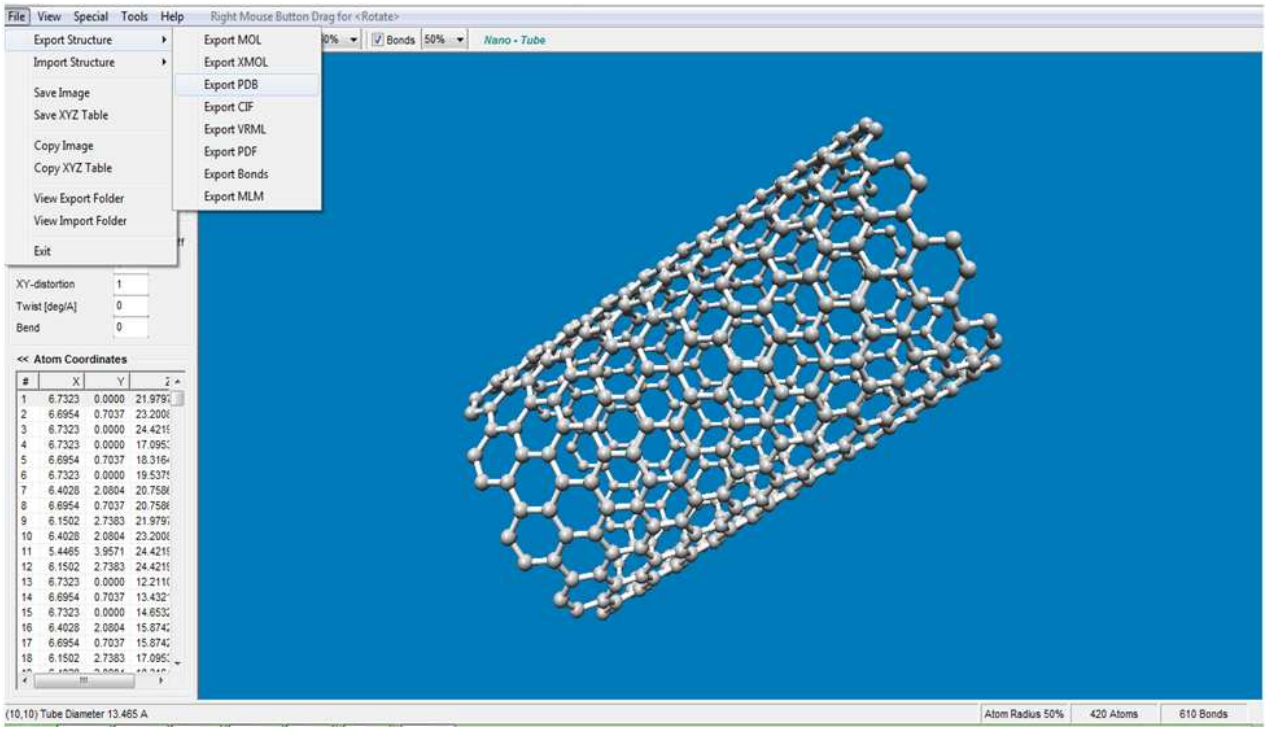

Figure 3.3: Exporting PDB file from Nanotube Modeler

```
REMARK    Nanotube Modeler PDB file (JCrystalSoft)
REMARK    Created:02-07-2012 17:22:46
CRYST1     1.000     1.000     1.000  90.00  90.00  90.00 P1
ATOM       1  C      C A   1        3.887   0.000   0.000  1.00  0.00
ATOM       2  C      C A   1        3.697   1.201   2.115  1.00  0.00
ATOM       3  C      C A   1        3.887   0.000   1.410  1.00  0.00
ATOM       4  C      C A   1        3.697   1.201   3.525  1.00  0.00
ATOM       5  C      C A   1        3.887   0.000   4.230  1.00  0.00
ATOM       6  C      C A   1        3.697   1.201   6.345  1.00  0.00
ATOM       7  C      C A   1        3.887   0.000   5.640  1.00  0.00
ATOM       8  C      C A   1        3.697   1.201   7.755  1.00  0.00
ATOM       9  C      C A   1        3.887   0.000   8.460  1.00  0.00
ATOM      10  C      C A   1        3.697   1.201  10.575  1.00  0.00
ATOM      11  C      C A   1        3.887   0.000   9.870  1.00  0.00
ATOM      12  C      C A   1        3.697   1.201  11.985  1.00  0.00
ATOM      13  C      C A   1        3.887   0.000  12.690  1.00  0.00
ATOM      14  C      C A   1        3.697   1.201  14.805  1.00  0.00
ATOM      15  C      C A   1        3.887   0.000  14.100  1.00  0.00
ATOM      16  C      C A   1        3.697   1.201  16.215  1.00  0.00
ATOM      17  C      C A   1        3.887   0.000  16.920  1.00  0.00
ATOM      18  C      C A   1        3.697   1.201  19.035  1.00  0.00
ATOM      19  C      C A   1        3.887   0.000  18.330  1.00  0.00
ATOM      20  C      C A   1        3.697   1.201  20.445  1.00  0.00
(TO BE CONTINUED FOR 240 ATOMS)
TER
CONECT    1    3
CONECT    2    3    4   27
CONECT    3    1    2  218
CONECT    4    2    5   29
CONECT    5    4    7  220
CONECT    6    7    8   31
CONECT    7    5    6  222
CONECT    8    6    9   33
CONECT    9    8   11  224
CONECT   10   11   12   35
CONECT   11    9   10  226
CONECT   12   10   13   37
CONECT   13   12   15  228
CONECT   14   15   16   39
CONECT   15   13   14  230
CONECT   16   14   17   41
CONECT   17   16   19  232
CONECT   18   19   20   43
CONECT   19   17   18  234
CONECT   20   18   21   45
CONECT   21   20   23  236
CONECT   22   23   24   47
CONECT   23   21   22  238
(TO BE CONTINUIED FOR ALL 240 ATOMS)
MASTER        0    0    0    0    0    0    0    0  240    0  240    0
END
```

Figure 3.4: Representation of information saved in pdb file

A typical pdb file describing a protein consists of hundreds to thousands of lines of carbon nanotube. Now we want to copy the coordinates of each atom and its connectivity. To do it manually it takes very long time so we have written a python script which will change the pdb file to ansys pre-processor file.

3.1.2.2 Generation of Ansys Pre Processor Script

We have generated a code which to convert pdb format into ansys pre-processor script. To execute the ansys script we use Wing IDE software which works as a compiler for python.

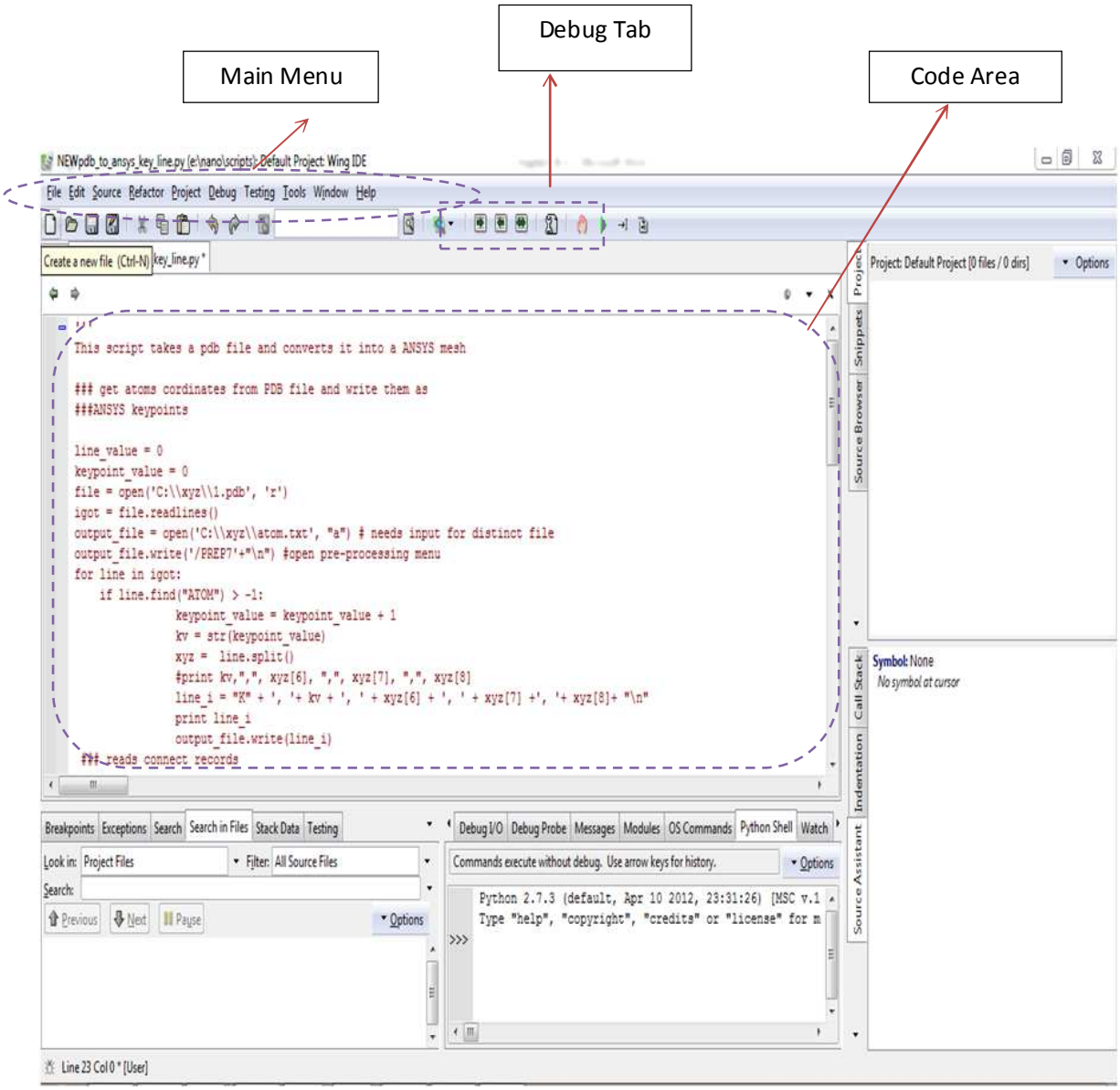

Figure 3.5: General layout of wing IDE software

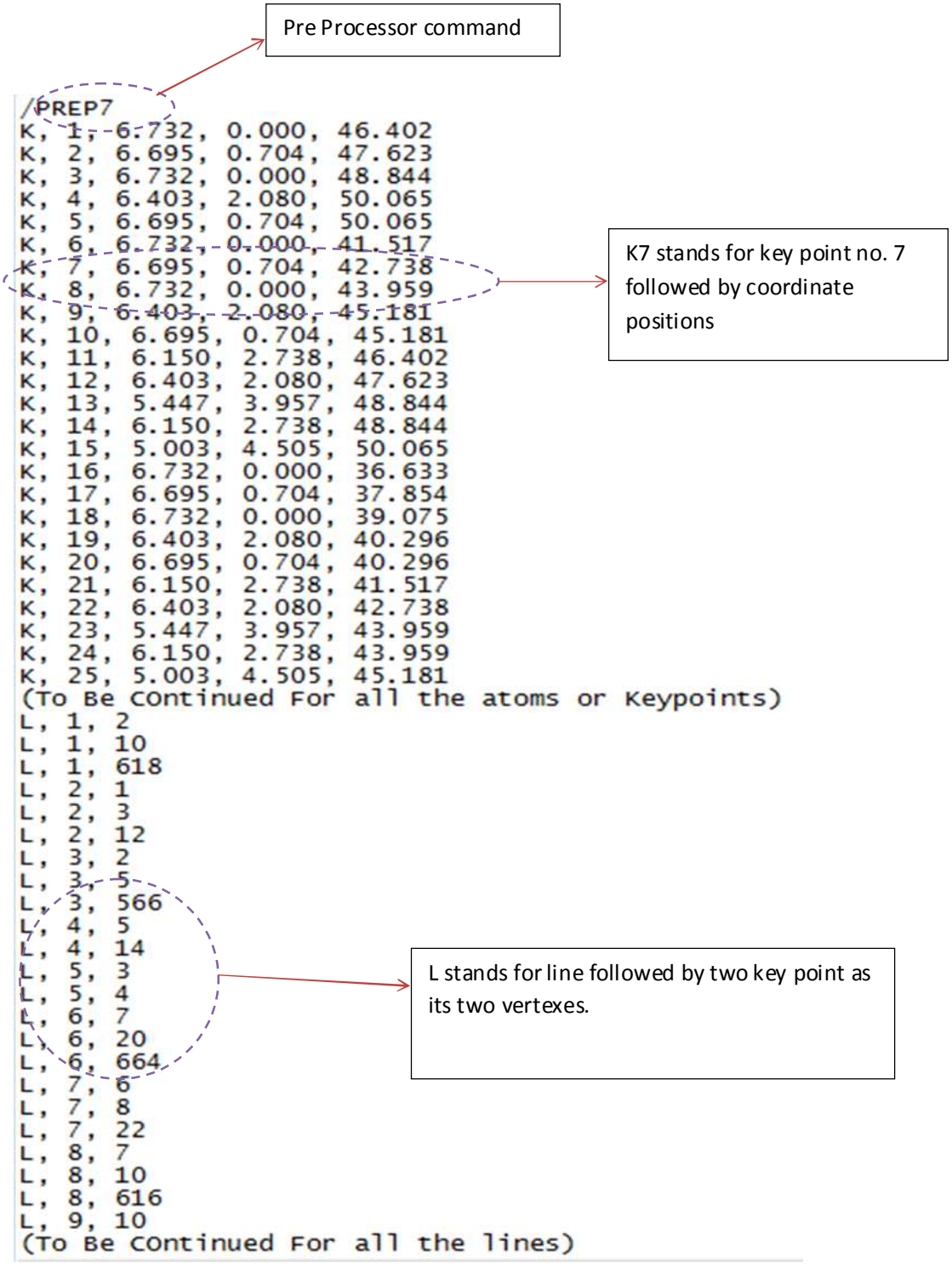

Figure 3.6: Representation of information saved in Ansys Script

By running this script in ansys Mechanical APDL command window we can draw the Nanotube in Ansys.

3.1.3 Wireframe Model of Carbon Nanotube in Ansys

By using the above explained method we have created three model of carbon nanotube of specification

1. n=10,m=0,lendth=5nm
2. n=10,m=8,length=5nm
3. n=10,m=10,length=5nm

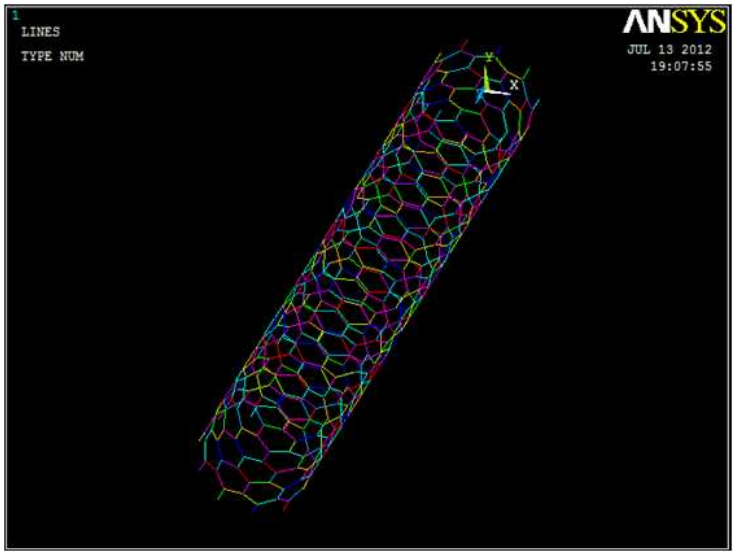

Figure 3.7 Ansys generated wireframe model of Nanotube(10,0) and 5 nm length

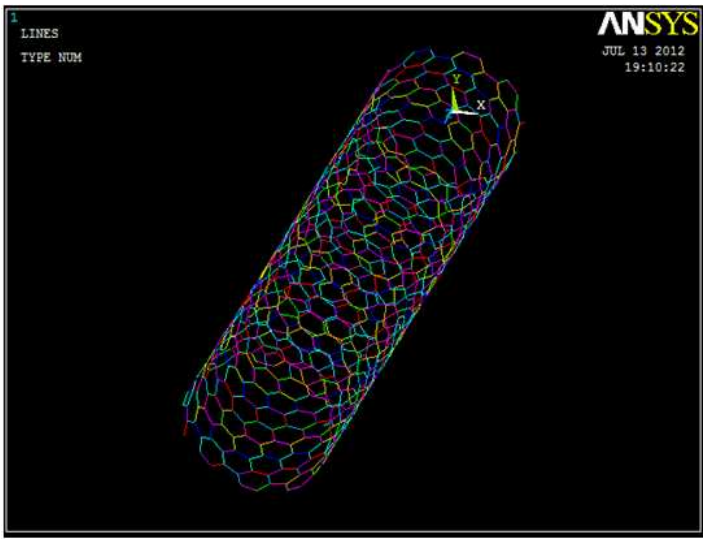

Figure 3.8 Ansys generated wireframe model of Nanotube(10,8) and 5 nm length

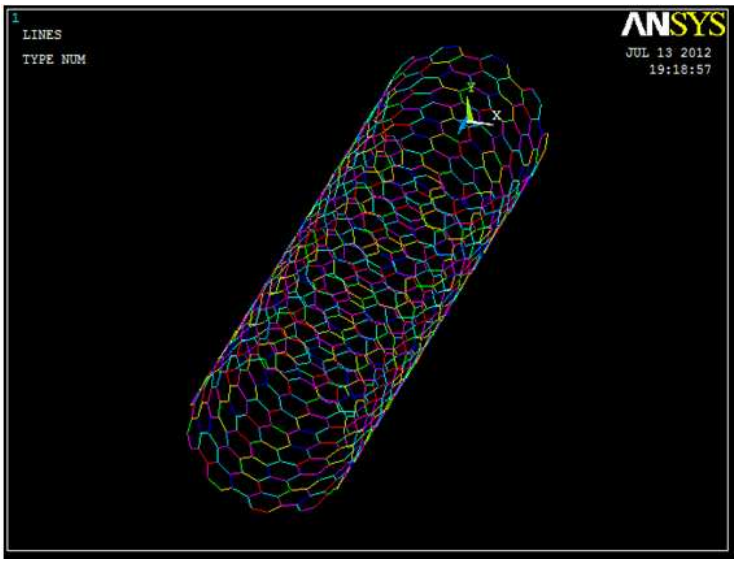

Figure 3.9 Ansys generated wireframe model of Nanotube(10,8) and 5 nm length

3.1.4 Selection of Type of Element

The C-C bond elements are modeled using BEAM4 element. BEAM4 is a uniaxial element with tension, compression, torsion, and bending as well as stress stiffening and large deflection capabilities. The element has six degrees of freedom at each node *x, y, z* nodal translational directions and rotations about the nodal *x, y, z* axis . The specifics of BEAM4 are displayed in Fig. 3.10. In the analysis, the nodes become the carbon atoms while the elements represent the bonds. For this reason, the elements are meshed with zero divisions. Moreover we can divide the elements into no of parts we want so as to accurate our results.

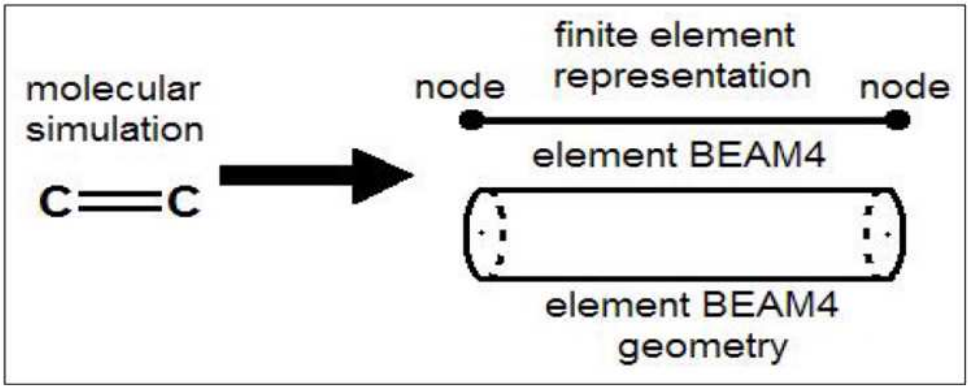

Figure 3.10: Representation of C-C bond in a molecular simulation as well as finite element modeling.

3.1.4.1 Basic Geometry and Input Parameters of Element

The geometry, node locations, and coordinate systems for this element are shown in fig 3.11. The element is defined by two or three nodes, the cross-sectional area, two area moments of inertia (I_{ZZ} and I_{YY}), two thicknesses (TKY and TKZ), an angle of orientation (Θ) about the element x-axis, the torsional moment of inertia (I_{XX}), and the material properties. If I_{XX} is not specified or is equal to 0.0, it is assumed equal to the polar moment of inertia ($I_{YY}+I_{ZZ}$). I_{XX} should be positive and is usually less than the polar moment of inertia. The element torsional stiffness decreases with decreasing values of I_{XX}.

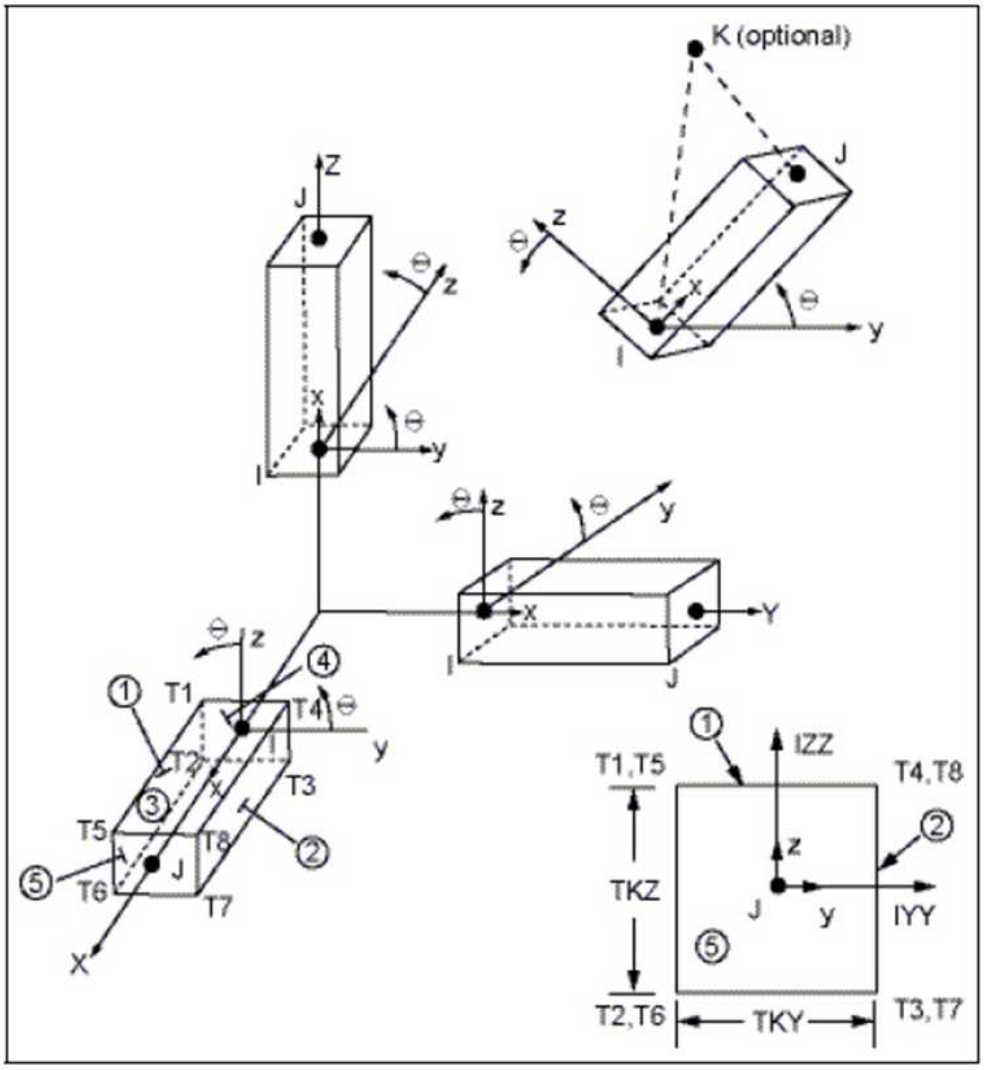

Figure 3.11: Geometric characteristics presented in element BEAM4 employed in ANSYS to construct the space-frame model of carbon nanotube

Table2: Input Values for BEAM 4 Element

Author	Tkz=Tky	Area($Å^2$)	$I_{XX}(Å^4)$	$I_{YY}(Å^4)$	$I_{ZZ}(Å^4)$
Tserpes & Papanikos[7]	1.470	1.6972	.2292	.2292	.4584
Kudin et al[25]	.890	.6221	.3080	.3080	.0616
Pantano et al.[27]	.750	.4418	.01554	.01554	.03106
Chen & Cao[26]	.500	.1963	.003068	.0030668	.006136

3.1.5 Nodes and Elements Calculation

We have to define single nodes at each key points because in our model the atoms are at the place of nodes and we have created key points at the coordinates of each atom. So we pick all points to create nodes.

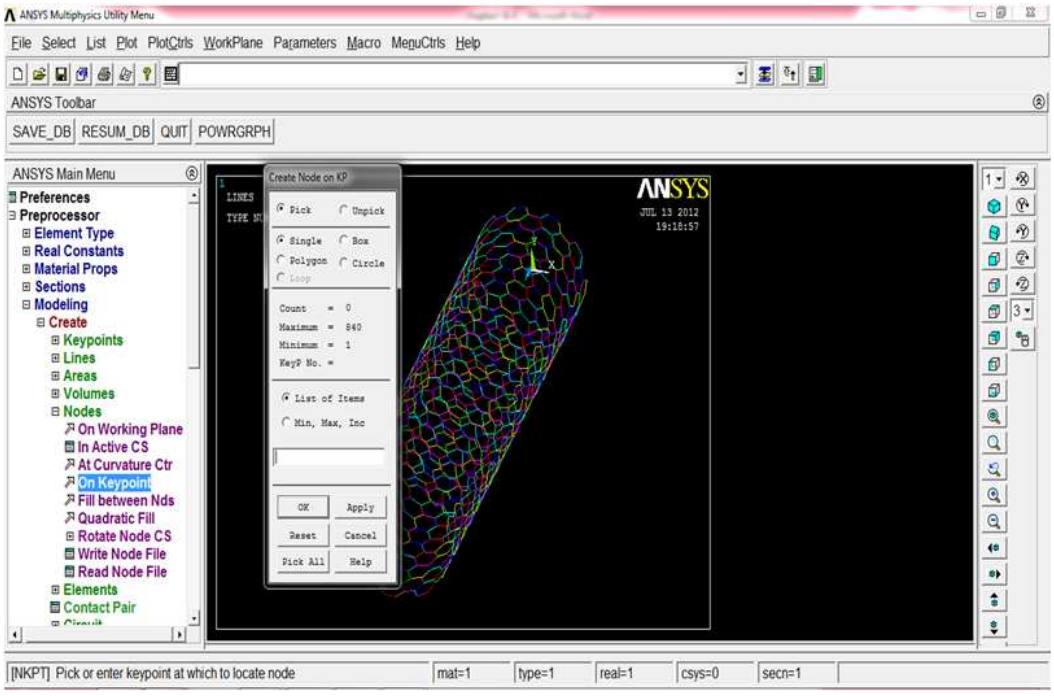

Figure 3.12 Representation of creation of nodes on keypoints in Ansys

After selecting pick all point sfrom the menu the Software will automatically generate nodes at the place of keypoints as shown in figure 3.13.

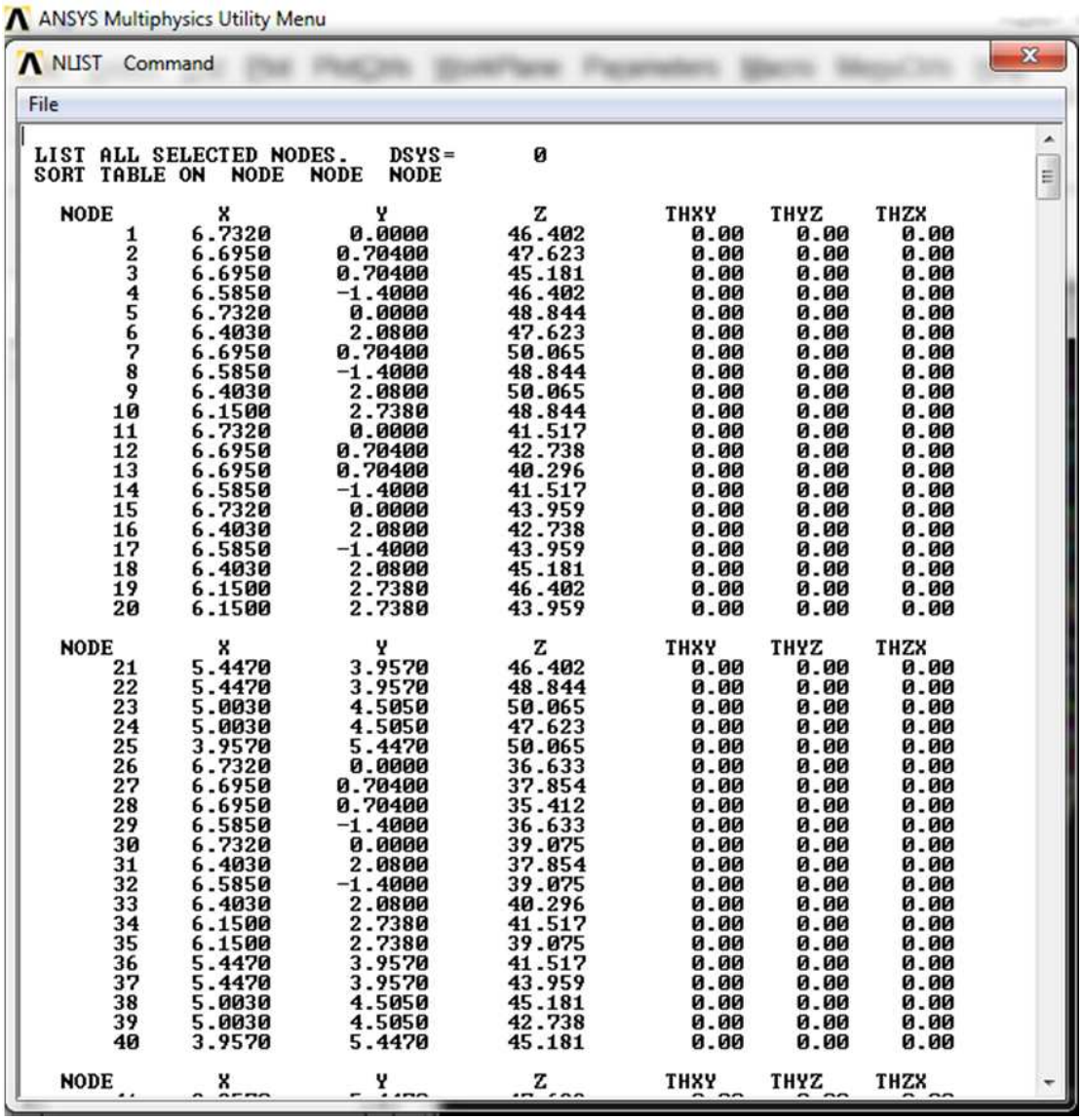

Figure 3.13 : Text file containing all nodes information generated by ansys

Table 3: Calculation of Nodes and Elements

Structure of Nanotube(n,m)	Length(nm)	No of Nodes	No of Elements (if elements is divided in single part)	No of Elements (if elements is divided in two part)
(10,0)	10	950	1410	2820

(10.5)	10	1255	1865	3730
(10,10)	10	1659	2468	4936
(8,0)	8	608	896	1792
(8,5)	8	883	1280	2560
(8,8)	8	1056	1568	3136
(5,0)	5	240	350	700
(5,3)	5	334	492	984
(5,5)	5	420	620	1240

3.1.6 Material Properties of Carbon Nanotube in Ansys

We have input material properties to begin our analsys. We consider carbon nanotube as linear elastic material. Material properties from different literature have been investigated and finally we have decided to input following values.

Table 4 : Material Properties of Carbon Nanotube

Serial No	Property	Symbol in Ansys	Value	Units
1	Young/s Modulus	EX	88.76	Kg $Å^{-1}S^{-2}$
2	Density	DENS	2.68×10^{-27}	$Kg/Å^3$
3	Poisson's Ratio	PRXY	.19	No units

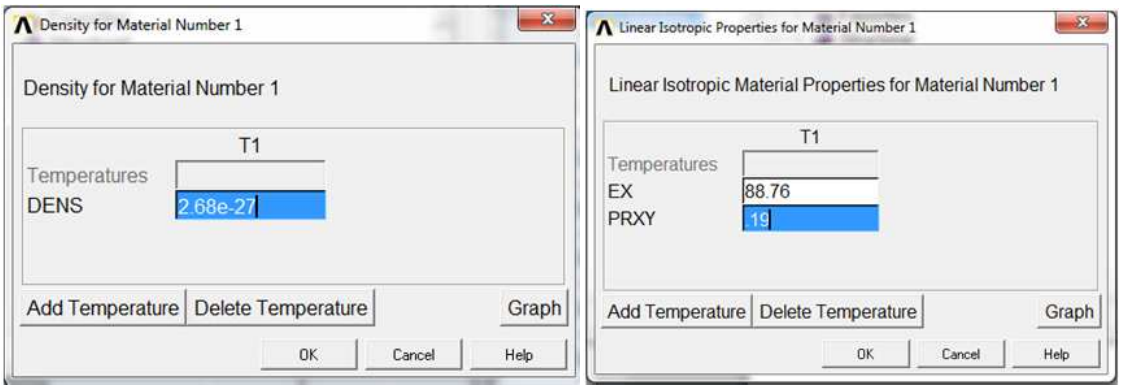

Figure 3.14 : Material Properties input window in Ansys

3.1.7 Meshing of Wireframe Model

Basically there are four ways by which we can do meshing:

1. Point Meshing
2. Line Meshing
3. Area Meshing
4. Volume Meshing

Since we have wireframe model so we have chosen line meshing .We have divided each line into one and two no of elements consecutively.

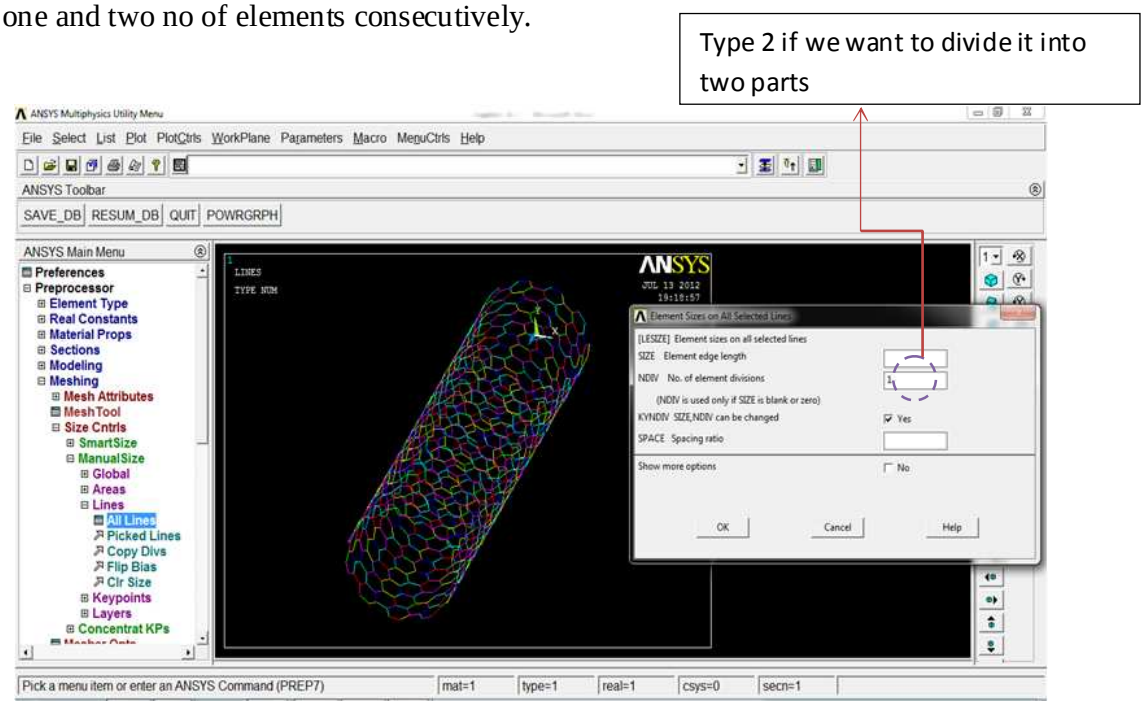

Figure 3.15: Representation of meshing attributes in Ansys

3.1.8 Loading Conditions and Boundary Constraints in Carbon Nanotube

There are basically two type of boundary constraints:

1. Fixed-Fixed (Both the ends of carbon nanotube are fixed)
2. Fixed-Free(One end of nanotube is fixed while other is free)

Load can be applied to any nodes in one of the *x-y-z* direction. A load of 10-27 Kg have been applied at all the nodes in between the center of the nanotube in downward direction i.e. negative Y direction.

To define a modal analsys we have to define the no of modes for frequency**.** We have chosen five modes of vibration. Either the software itself will decide the frequency or we can also input.

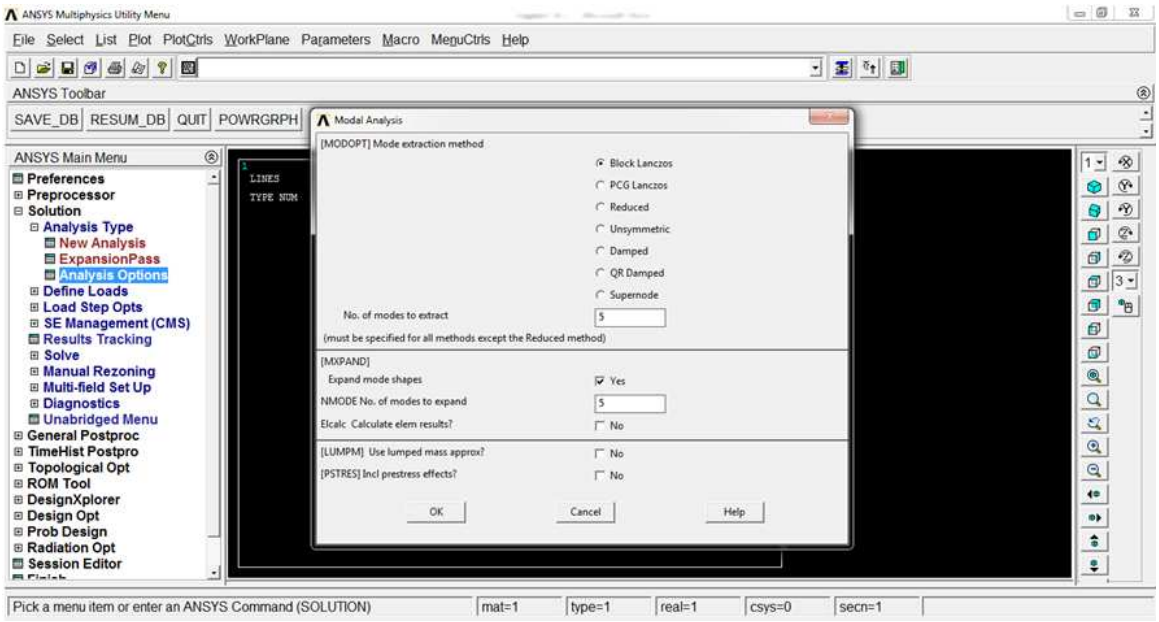

Figure 3.16: Basics input parameters for modal analyses

CHAPTER 4

RESULTS AND DISCUSSIONS

4.1 NORMAL SIMULATION

Initially Simulation has to run in Ansys 13.0 . There are total six simulations has to run by changing geometric and process parameters from job 1 to job 8 explained in table. For all these simulation, the same material properties used as explained in table.

Table 5: Nanotube Structures and plans for Simulation

Job Number	(n, m)	Length(nm)	Boundary Conditions	Load Conditions	No of elements per line
1	(10,10)	5	Fixed-Fixed	At center	1
			Fixed- Free	At free end	
2	(10,0)	5	Fixed-Fixed	At center	1
			Fixed- Free	At free end	
3	(10,10)	5	Fixed-Fixed	At center	2
			Fixed- Free	At free end	
4	(10,0)	5	Fixed-Fixed	At center	2
			Fixed- Free	At free end	
5	(5,5)	5	Fixed-Fixed	At center	1
			Fixed- Free	At free end	
6	(5,0)	5	Fixed-Fixed	At center	1
			Fixed- Free	At free end	
7	(5,5)	5	Fixed-Fixed	At center	2
			Fixed- Free	At free end	
8	(5,0)	5	Fixed-Fixed	At center	2
			Fixed- Free	At free end	

4.1.1 Job 1: Simulation of carbon nanotube(10,10) and length 5nm

A carbon nanotube is modeled in Ansys 13.0 with n=10, m=10 and length 5nm. BEAM 4 type element is used and $T_{kz} = T_{ky} = 1.470$ Å as showed in table 2. Material properties are used from table 4. A load of 10^{-24} Kg is applied in two ways showed in table 5.Total 6 natural frequencies are found and 6 mode shapes are drawn.

Table 6: Index of data sets on Nanotube (10, 10) and length 5nm Fixed-Fixed without load

Set	Frequency(Hz)	Load set	Sub set	Cumulative
1	0.40020E+12	1	1	1
2	0.40020E+12	1	2	2
3	0.54306E+12	1	3	3
4	0.54306E+12	1	4	4
5	0.65668E+12	1	5	5
6	0.73474E+12	1	6	6

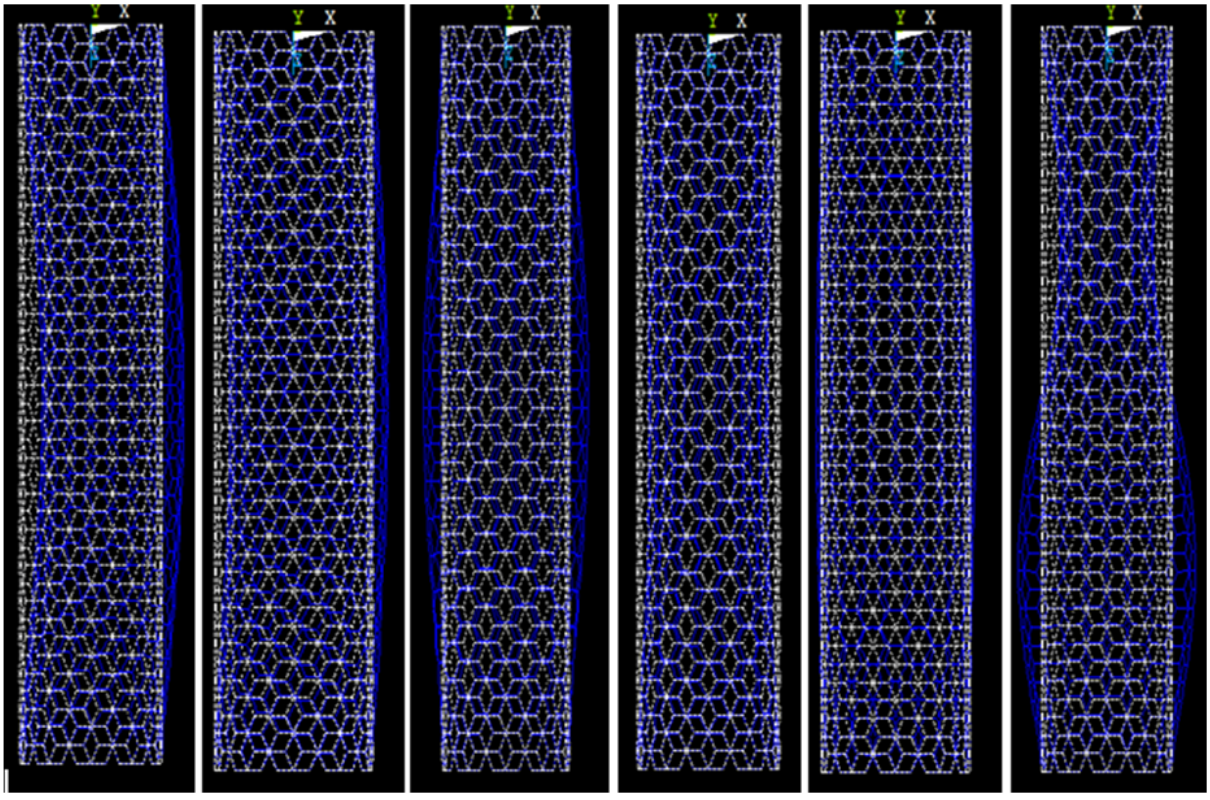

Figure 4.1 : Modes shapes of Nanotube (10, 10) and length 5nm Fixed-Fixed without load

Table 7: Index of data sets on Nanotube (10, 0) and length 5nm Fixed-Free without load

Set	Frequency(Hz)	Load set	Sub set	Cumulative
1	0.10058E+12	1	1	1
2	0.10058E+12	1	2	2
3	0.32409E+12	1	3	3
4	0.43008E+12	1	4	4
5	0.43008E+12	1	5	5
6	0.49131E+12	1	6	6

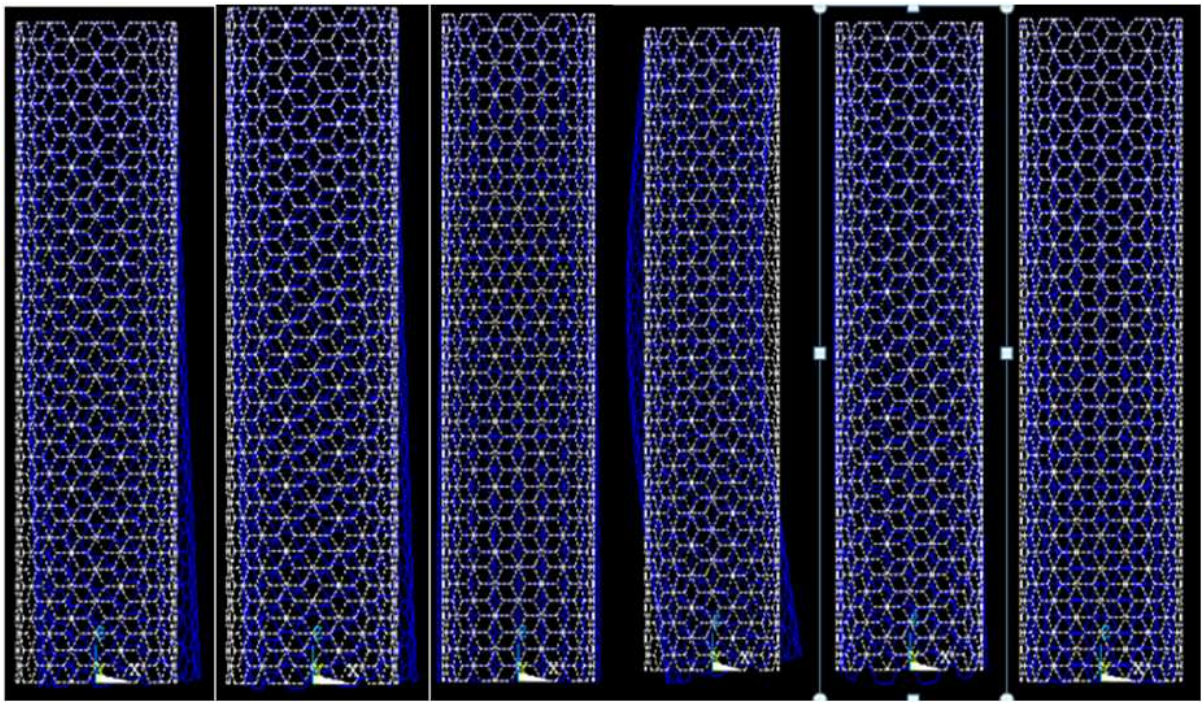

Figure 4.2 : Modes shapes of Nanotube (10, 10) and length 5nm Fixed-Free without load

4.1.2 Job 2: Simulation of carbon nanotube(10,0) and length 5nm

A carbon nanotube is modeled in Ansys 13.0 with n=10, m=0 and length 5nm. BEAM 4 type element is used and $T_{kz} = T_{ky} = 1.470$ Å as showed in table 2. Material properties are used from table 4. A load of 10^{-24} Kg is applied in two ways showed in table 5.Total 6 natural frequencies are found and 6 mode shapes are drawn.

Table 8: Index of data sets on Nanotube (10, 0) and length 5nm Fixed-Fixed without load

Set	Frequency(Hz)	Load set	Sub set	Cumulative
1	0.32256E+12	1	1	1
2	0.32256E+12	1	2	2
3	0.66040E+12	1	3	3
4	0.72525E+12	1	4	4
5	0.72525E+12	1	5	5
6	0.10620E+13	1	6	6

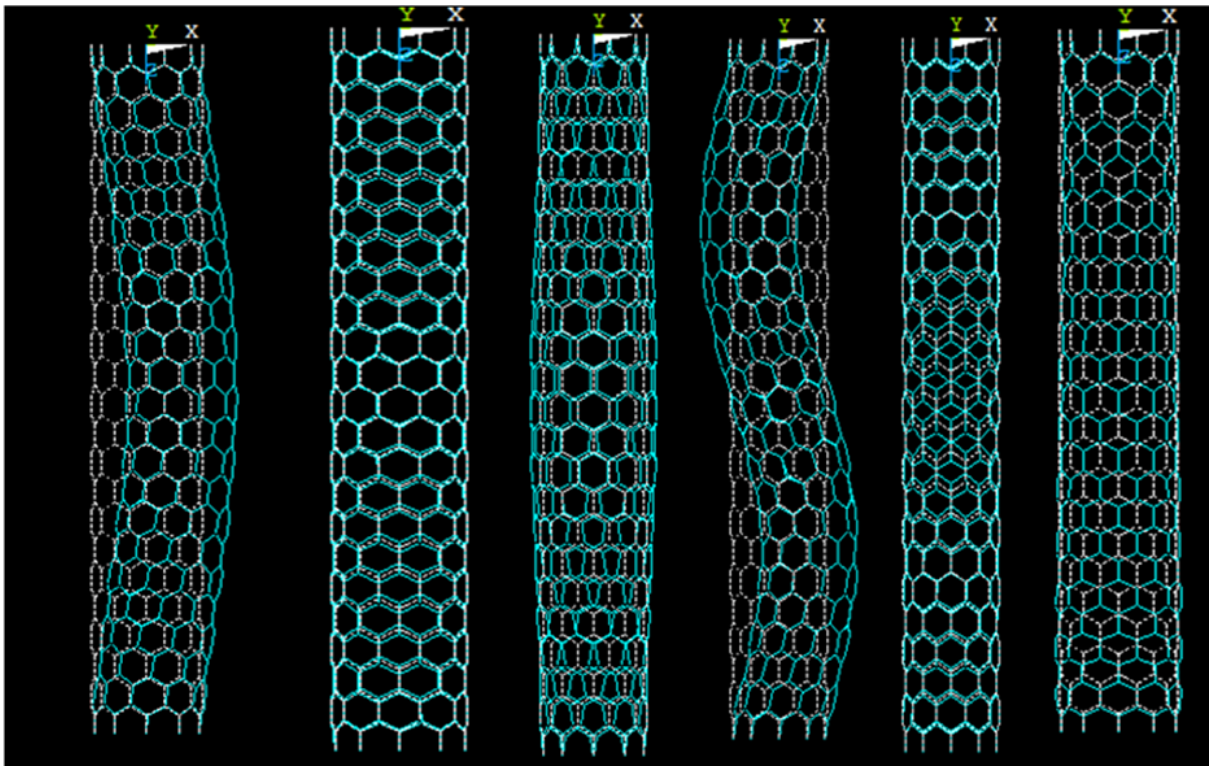

Figure 4.3 : Modes shapes of Nanotube (10, 0) and length 5nm Fixed-Fixed without load

Table 9: Index of data sets on Nanotube (10, 0) and length 5nm Fixed-Free without load

Set	Frequency(Hz)	Load set	Sub set	Cumulative
1	0.64172E+11	1	1	1
2	0.64172E+11	1	2	2
3	0.33130E+12	1	3	3

4	0.33641E+12	1	4	4
5	0.33641E+12	1	5	5
6	0.53261E+12	1	6	6

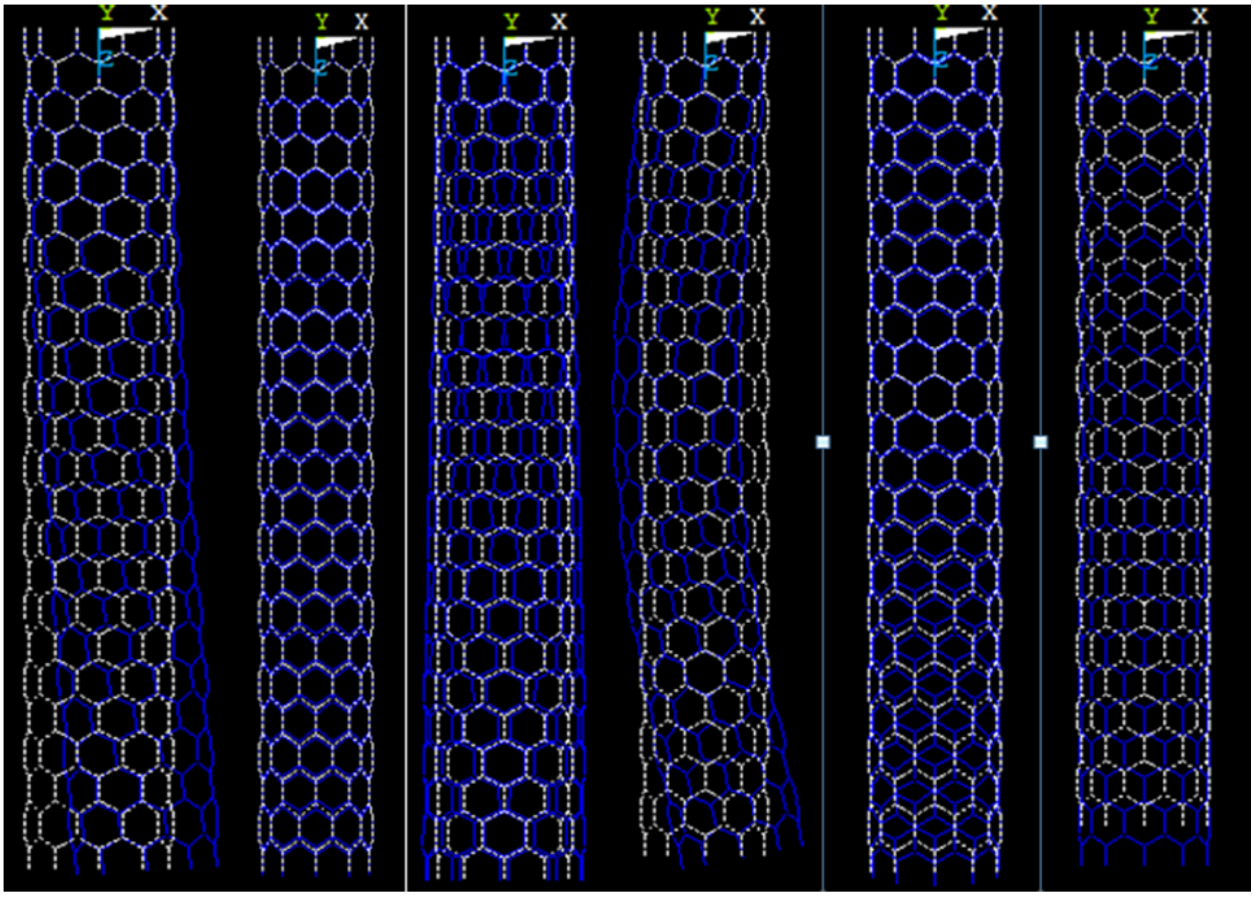

Figure 4.4 : Modes shapes of Nanotube (10, 0) and length 5nm Fixed-Free without load

4.1.3 Job 3: Simulation of carbon nanotube(5,5) and length 5nm

A carbon nanotube is modeled in Ansys 13.0 with n=5, m=5 and length 5nm. BEAM 4 type element is used and $T_{kz} = T_{ky} = 1.470$ Å as showed in table 2. Material properties are used from table 4. A load of 10^{-24} Kg is applied in two ways showed in table 5.Total 6 natural frequencies are found and 6 mode shapes are drawn.

Table 10: Index of data sets on Nanotube (5,5) and length 5nm Fixed-Fixed without load

Set	Frequency(Hz)	Load set	Sub set	Cumulative
1	0.29363E+12	1	1	1

2	0.29363E+12	1	2	2
3	0.65861E+12	1	3	3
4	0.67793E+12	1	4	4
5	0.67793E+12	1	5	5
6	0.10605E+13	1	6	6

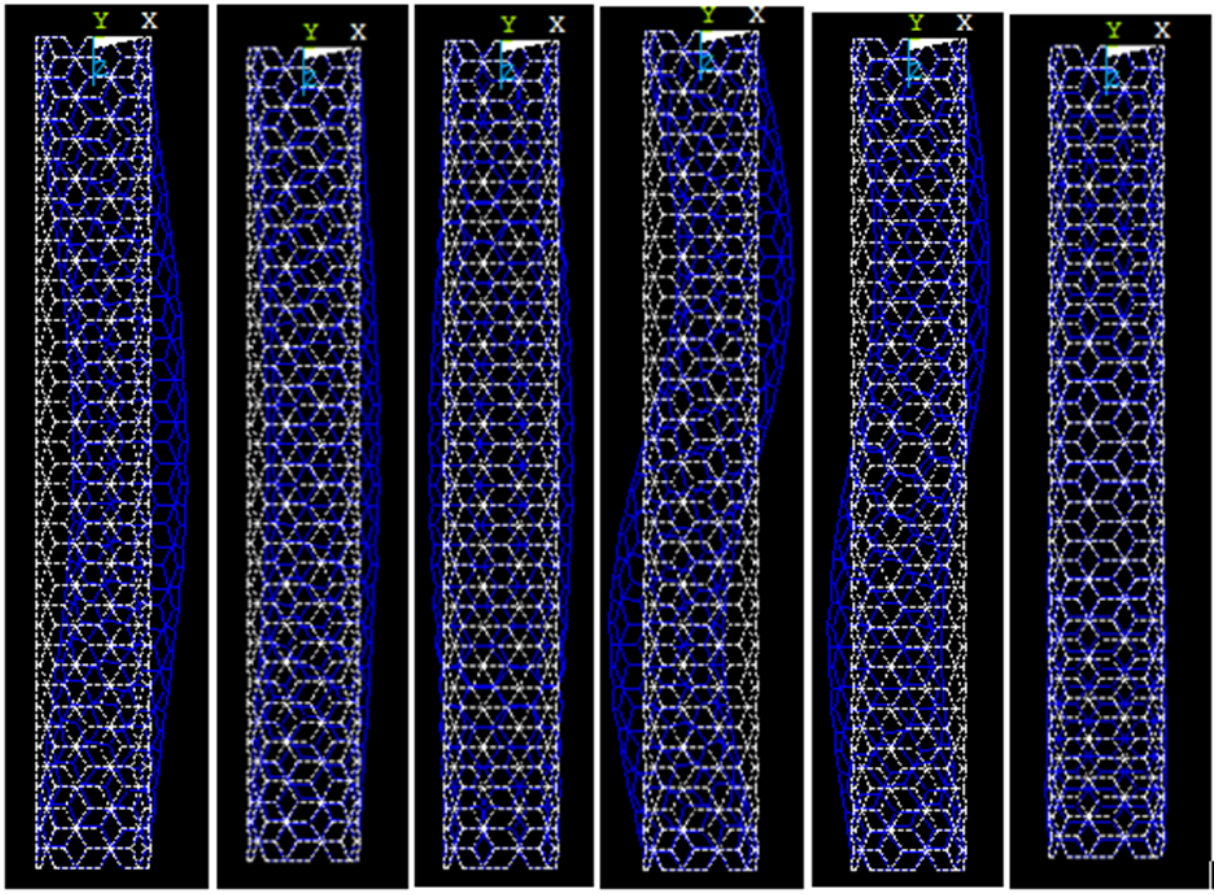

Figure 4.5 : Modes shapes of Nanotube (5,5) and length 5nm Fixed-Fixed without load

Table 11: Index of data sets on Nanotube (5,5) and length 5nm Fixed-Free without load

Set	Frequency(Hz)	Load set	Sub set	Cumulative
1	0.55257E+11	1	1	1
2	0.55257E+11	1	2	2
3	0.29946E+12	1	3	3
4	0.29946E+12	1	4	4

5	0.32509E+12	1	5	5
6	0.52685E+12	1	6	6

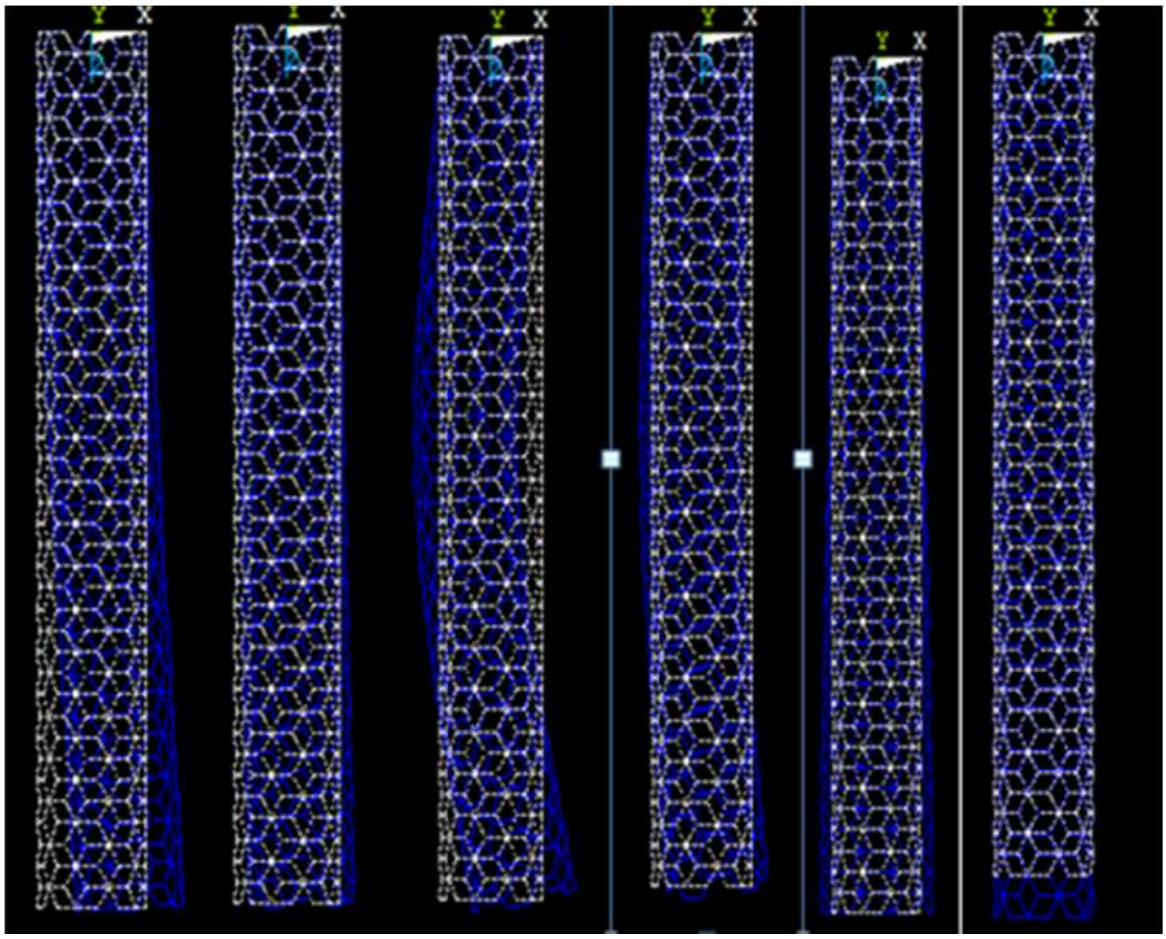

Figure 4.6 : Modes shapes of Nanotube (5,5) and length 5nm Fixed-Free without load

4.1.4 Job 4: Simulation of carbon nanotube(5,0) and length 5nm

A carbon nanotube is modeled in Ansys 13.0 with n=5, m=0 and length 5nm. BEAM 4 type element is used and $T_{kz} = T_{ky} = 1.470$ Å as showed in table 2. Material properties are used from table 4. A load of 10^{-24} Kg is applied in two ways showed in table 5.Total 6 natural frequencies are found and 6 mode shapes are drawn.

Table 12: Index of data sets on Nanotube (5,0) and length 5nm Fixed-Fixed without load

Set	Frequency(Hz)	Load set	Sub set	Cumulative
1	0.32597E+11	1	1	1
2	0.33395E+11	1	2	2
3	0.19985E+12	1	3	3
4	0.19989E+12	1	4	4
5	0.34493E+12	1	5	5
6	0.52607E+12	1	6	6

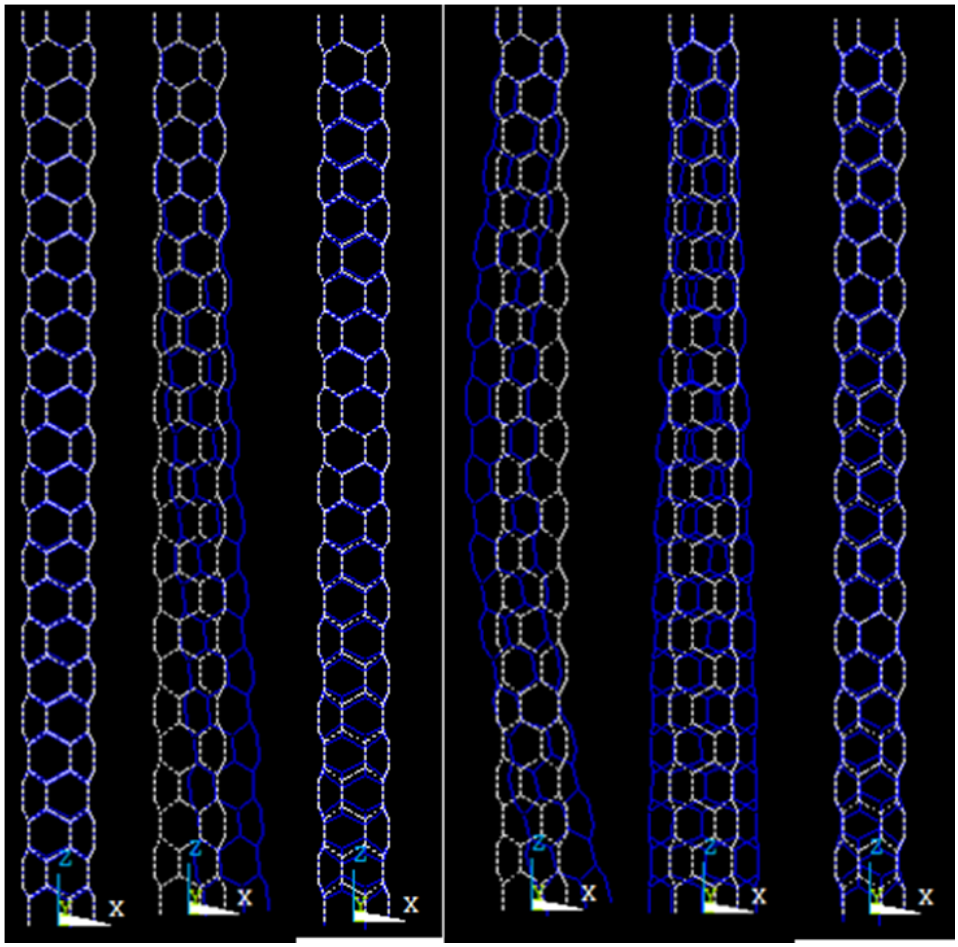

Figure 4.7 : Modes shapes of Nanotube (5,5) and length 5nm Fixed-Fixed without load

Table 13: Index of data sets on Nanotube (5,0) and length 5nm Fixed-Free without load

Set	Frequency(Hz)	Load set	Sub set	Cumulative
1	0.33388E+11	1	1	1
2	0.33395E+11	1	2	2
3	0.19985E+12	1	3	3
4	0.19985E+12	1	4	4
5	0.34493E+12	1	5	5
6	0.52607E+12	1	6	6

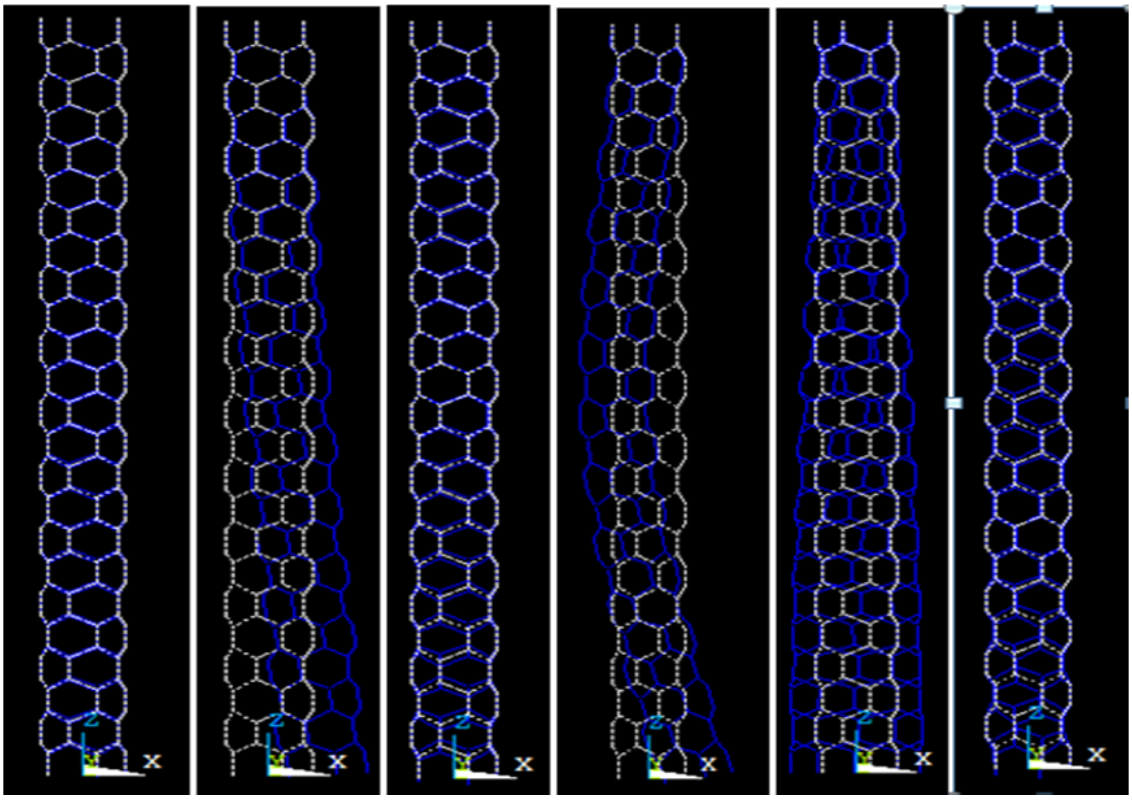

Figure 4.8 : Modes shapes of Nanotube (5,0) and length 5nm Fixed-Free without load

4.2 Study the Change in Frequency by Appling Load on Carbon Nanotube

All the modes obtained in section 4.1 are without the application of any load if we apply load to any carbon nanotube, a significant change in natural frequency of the carbon nanotube has been observed. We can detect the mass by calculating the natural frequency of nanotube(10,10) as fixed-fixed condition.

Table 14 : Natural frequency with change in length and mass

Serial No	Attached Mass(Kg)	Natural Frequency(HZ)			
		Length = 6nm	Length = 8nm	Length = 10nm	Length = 12nm
1	10^{-26}	9.89E+10	7.31E+10	5.89 E+10	4.17 E+10
2	10^{-25}	9.62 E+10	7.06 E+10	5.56 E+10	3.96 E+10
2	10^{-24}	6.42 E+10	5.36 E+10	4.46 E+10	2.76 E+10
2	10^{-23}	2.35 E+10	2.15 E+10	1.84 E+10	1.35 E+10
5	10^{-22}	3.59 E+09	2.75 E+09	2.56 E+09	2.02 E+09
6	10^{-21}	2.45 E+08	2.23 E+08	1.93 E+08	9.96 E+07
7	10^{-20}	5.99 E+07	4.16 E+07	3.32 E+07	1.3 E+07

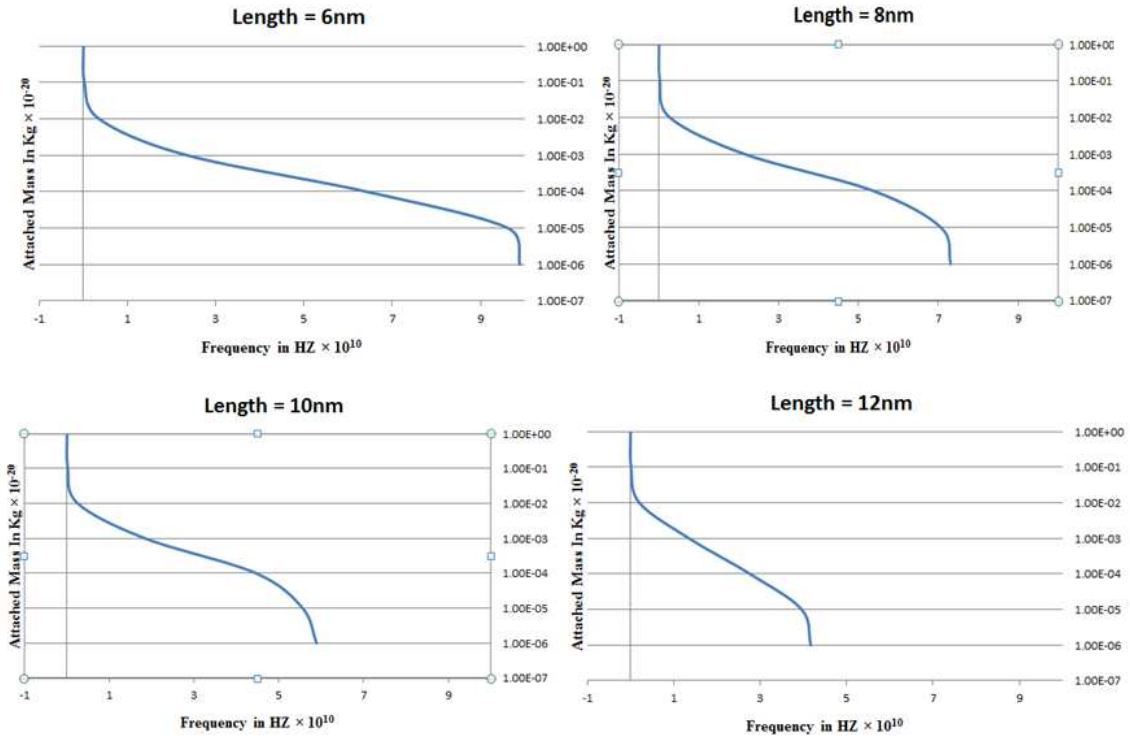

Figure 4.9 : Graphical Representation of Natural Frequency by varing tube length

By ploting all the data on single graph we can determine the freuency shift of carbon nano tube by chaning the value of attached mass to it. So by observing this signature we can find the amount of mass attached to nanotube.

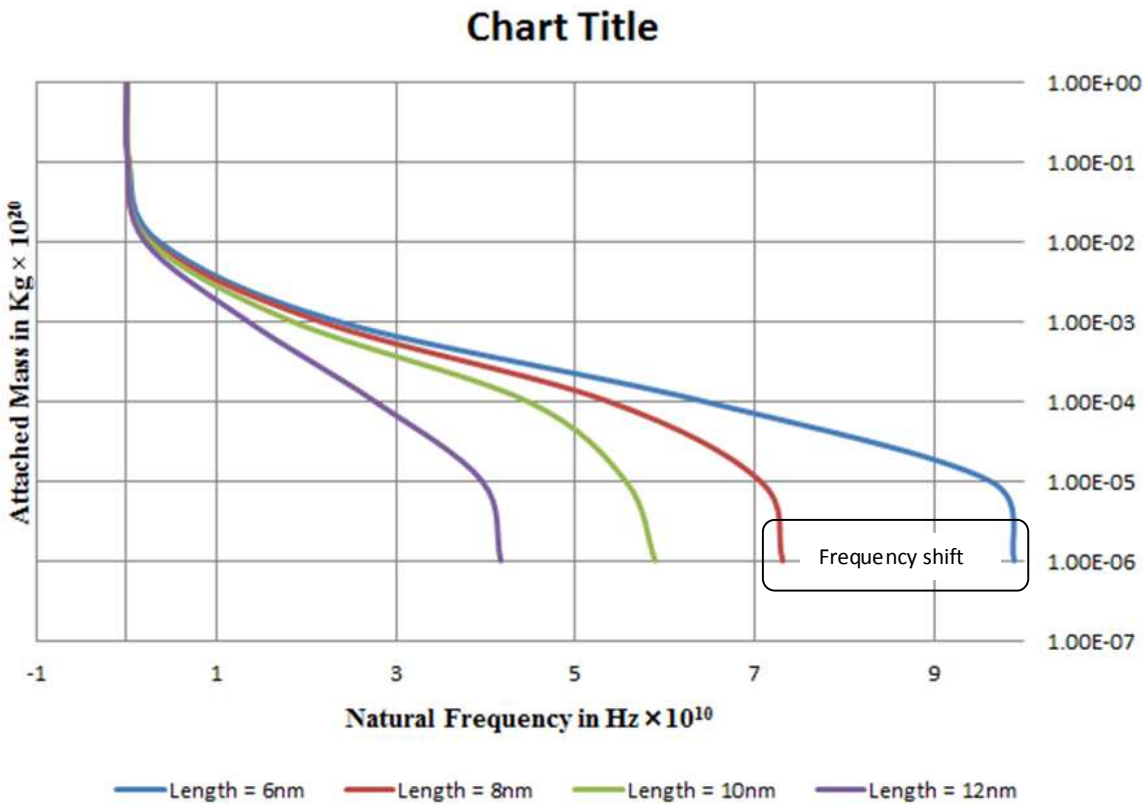

Figure 4.10 : Graphical Representation of Shift in Natural Frequency

4.3 Study the Change in Frequency by Aspect Ratio of Carbon Nanotube

We have observed the natural frequency of carbon nanotube by changing its length to diameter ratio.

Table 15 : Natural frequency with change in length to diameter ratio

Serial Number	(n,m)	Length(nm)	Diameter(nm)	*l/D*	Natural Frequency (Hz)
1	(10,10)	10	1.34	7.46	4.2E10
2	(10,0)	10	.77	12.98	3.5E10
3	(10,5)	10	1.02	9.80	3.88E10
4	(10,10)	20	1.34	14.92	2.8E10
5	(10,0)	20	.77	25.97	1.1E10
6	(10,5)	20	1.02	19.60	1.3E10

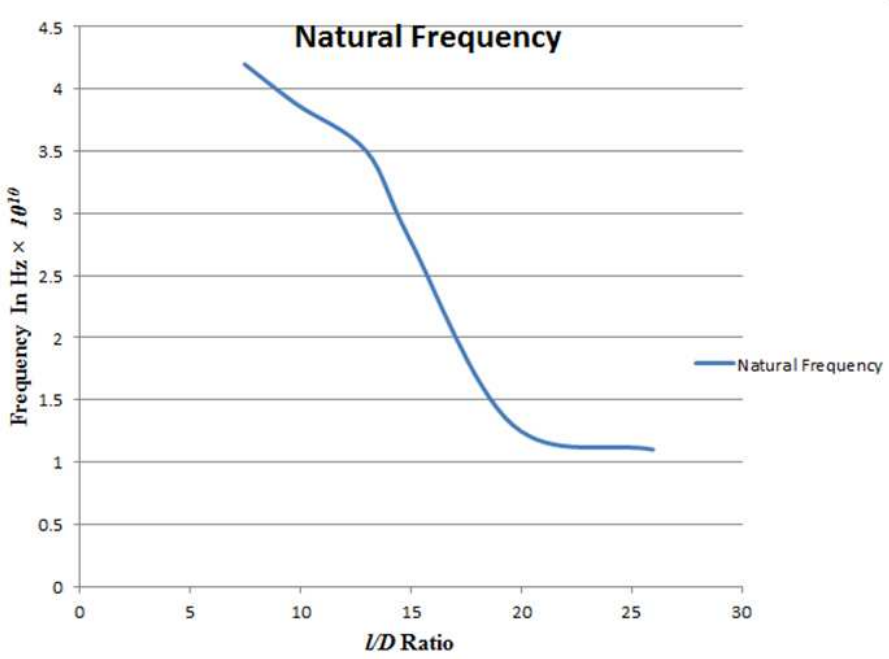

Figure 4.11 : Graphical Representation of Natural Frequency by varing aspect ratio

As clearly shown by graph it is observed that the natural frequency of carbon nanotube decreases with increase in l/D ratio. Smaller nanotubes can be used for obtaining high resonant frequency and vice versa.

CHAPTER 5

CONCLUSION AND FUTURE SCOPE

5.1 Conclusion

The main properties that make carbon nanotubes (CNTs) a promising technology for many future applications are: extremely high strength, low mass density, linear elastic behavior, almost perfect geometrical structure, and nanometer scale structure. Also, CNTs can conduct electricity better than copper and transmit heat better than diamonds. Therefore, they are bound to find a wide and possibly revolutionary use in all fields of engineering.

The present work analyzes the natural frequency of carbon nanotubes with and without loadings under fixed-fixed and fixed-free conditions. We have observed that there is significant change in the natural frequency after application of load on carbon nanotubes. So by observing the natural frequency of any nanotube we can find the force applied to it. Hence we can use carbon nanotube as a mass detector.

The results indicate that the mass sensitivity of carbon nanotube based mass detectors can reach 10^{-24} Kg and above. It has been observed that CNT with attached mass of 10^{-28} to 10^{-23} Kg, the clear peak of excitation appears at natural frequency and other peaks are at multiples of natural frequency.

With the help of this model we can draw the vibration signature of specific nanotube and find the peaks to identify which type of carbon nanotube is best for detecting specific amount of mass.

The accuracy of the model has been verified with the research work done by other authors.

5.1 Future Scope

The carbon nanotube resonates at 2 GHz. It can be studided that when the heavier masses with lower resonant frequency land on the carbon nanotube it lower its natural frequency, with heavier particles lowering it more than lighter ones. The shift in resonant frequency can be monitored and so be used to calculate the mass of the particle.

Such high frequency mechanical Nano devices will facilitate the development of the fastest scanning probe microscopes, magnetic resonant force microscopes, and even mechanical super-computers.

Since the carbon nanotube can detect very small mass so this carbon nanotube mass detector has wide application in biotechnology so as to measure the bacteria mass and many other parameters.

Present method of drawing model can also be used to draw the DNA structures and nanotubes of other material than carbon on any simulation software.

REFERENCES

[1] S.Iijima. Helical microtubules of graphitic carbon, Nature, vol. 354:56-58, 1991.

[2]http://www.directionsmag.com/articles/nanotechnology-and-the-fight-against-terrorism/123894 (01/06/2012

[3] http://www.nasa.gov/centers/langley/business/tg-img-nanopix.html(01/06/2012)

[4] http://en.wikipedia.org/wiki/Carbon_nanotube(02/06/2012)

[5] http://www.nanocyl.com/en/CNT-Expertise-Centre/Carbon-Nanotubes(02/06/2012)

[6] R. Saito, G. Dresselhaus, and M.S. Dresselhaus. Physical Properties of Carbon Nanotubes. Imperial College Press, London, UK, 1999.

[7] K.I. Tserpes and P. Papanikos. Finite element modeling of single-walled carbon nanotubes. Composites Part B, 2005.

[8] J. Han. Structures and properties of carbon nanotubes.

[9] A.P. Moravsky, E.M. Wexler, and R.O. Loutfy. Growth of carbon nanotubes by arc discharge and laser ablation.

[10] M. Cinke, J. Li, and et. al. Pore structure of raw and puri.ed hipco single-walled carbon nanotubes. Chemical Physics Letters, 365:69.74, 2002.

[11] P. Laborde-Lahoz, W. Maser, and et. al. Mechanical characterization of carbon nanotube composite materials. Mechanics of Advanced Materials, 2005.

[12] C. Kittel. Energy bands. In Introduction to Solid State Physics. John Wiley and Sons, Inc., New York, NY, 1986.

[13] E.H. Dill. Formulation of the finite element method for linear elasticity. In The Finite Element Method for the Mechanics of Solids.

[14] R. Ansari, S.Rouhi "Atomistic finite element model for axial buckling of single-walled carbon nanotubes" Published at Science Direct on June 17 2010 .

[15] Anand Y.Joshi , S.P.Harsha, Satish C.Sharma "Vibration signature analysis of single walled carbon nanotube based nanomechanical sensors" Published at Science Direct on March 25 2010 .

[16]. Mira Mitraa, S. Gopalakrishnan "Wave propagation in multi-walled carbon nanotube" Nanotechnology 17 (2006) 45–53.

[17] S.K. Georgantzinos, G.I. Giannopoulos, N.K. Anifantis "Investigation of stress–strain behavior of single walled carbon nanotube/rubber composites by a multi-scale finite element method" Published at Theoretical and Applied Fracture Mechanicson October 12 2009.

[18] S. Rajasekaran and P. Chitra "Structural Mechanics Approach for Carbon Nanotubes" Published at KSCE Journal of Civil Engineering (2009) 13(5):347-358 DOI 10.1007/s12205-009-0347-6.

[19] Aleksander Muc "Design and identification methods of effective mechanical properties for carbon nanotubes" Published at "Material and Design" on March 25, 2009

[20]. P. Zhang, Y. Huang, H. Gao, K.C. Hwang, J. Appl. Mech. Trans. ASME 69, 454 (2002)

[21]. P. Zhang, Y. Huang, P.H. Geubelle, P. Klein, K.C. Hwang, Int. J. Solids Struct. 39, 3893 (2002)

[22]. N. Khandoker, S.C. Hawkins, R. Ibrahim, C. P. Huynh, F. Deng "Tensile Strength of Spinnable Multiwall Carbon Nanotubes" Published at Science Direct Procedia Engineering 10 (2011) 2572–2578.

[23] R. Chowdhury, S.Adhikari, J.Mitchell "Vibrating carbon nanotube based bio-sensors" Published at Physica E 42 (2009) 104–109

[24]. B. Liu, H. Jiang, Y. Huang, S. Qu and M.-F. Yu "Atomic-scale finite element method in multiscale computation with applications to carbon nanotubes" Published at PHYSICAL REVIEW B 72, 035435 ,2005.

[25]. K.N. Kudin, G.E. Scuseria, and B.I. Yakobson. C, F, BN, and C nanoshell elasticity from ab initio computations. Phys. Rev, B, 64(23):235406, 2001.

[26] X. Chen and G. Cao. A structural mechanics study of single-walled carbon nanotubes generalized from atomistic simulation. Nanotechnology, 17:1004-1015, 2006.

[27] A. Pantano, D.M. Parks, and M.C. Boyce. Mechanics of deformation of single and multi-walled carbon nanotubes. J. Mech. Phys. Solids, 52:789-821, 2004.